Journal of Hazardous Materials 458 (2023) 131915

Contents lists available at ScienceDirect

Journal of Hazardous Materials

journal homepage: www.elsevier.com/locate/jhazmat

Research Paper

# Getting fat and stressed: Effects of dietary intake of titanium dioxide nanoparticles in the liver of turbot *Scophthalmus maximus*

Elza Fonseca [a,*], María Vázquez [b], Laura Rodriguez-Lorenzo [c], Natalia Mallo [b], Ivone Pinheiro [c], Maria Lígia Sousa [a], Santiago Cabaleiro [b], Monica Quarato [c], Miguel Spuch-Calvar [d], Miguel A. Correa-Duarte [d], Juan José López-Mayán [e], Mick Mackey [f], Antonio Moreda [e], Vítor Vasconcelos [a,g], Begoña Espiña [c], Alexandre Campos [a], Mário Jorge Araújo [a]

[a] *CIIMAR – Interdisciplinary Centre of Marine and Environmental Research, Terminal de Cruzeiros do Porto de Leixões, Av. General Norton de Matos s/n, 4450-208 Matosinhos, Portugal*
[b] *CETGA – Centro Técnológico del Cluster de la Acuicultura, Punta de Couso s/n, 15965 Ribeira, A Coruña, Spain*
[c] *INL – International Iberian Nanotechnology Laboratory, Av. Mestre José Veiga s/n, 4715-330 Braga, Portugal*
[d] *CINBIO – Centro de Investigación en Nanomateriais e Biomedicina, Universidade de Vigo, 36310 Vigo, Spain*
[e] *GETEE – Trace Element, Spectroscopy and Speciation Group, Institute de Materiais iMATUS. Faculty of Chemistry, University of Santiago de Compostela, Av. das Ciencias s/n, 15782 Santiago de Compostela, Spain*
[f] *IRMRC – Indigo Rock Marine Research Centre, Gearhies, Bantry, Co., Cork P75 AX07, Ireland*
[g] *FCUP – Faculty of Sciences, University of Porto, Biology Department, Rua do Campo Alegre s/n, 4169-007 Porto, Portugal*

## HIGHLIGHTS

- Dietary exposure to citrate-coated $TiO_2$ NPs was studied in turbot liver.
- The liver plays a key role in $TiO_2$ NPs accumulation, metabolization and excretion.
- The hepatic metabolism of turbots is affected regardless of $TiO_2$ NPs size.
- Smaller NPs drive hepatic steatosis, larger NPs lead to lipid droplets depletion.
- Lipids degradation contributes to oxidative stress and immune response activation.

## GRAPHICAL ABSTRACT

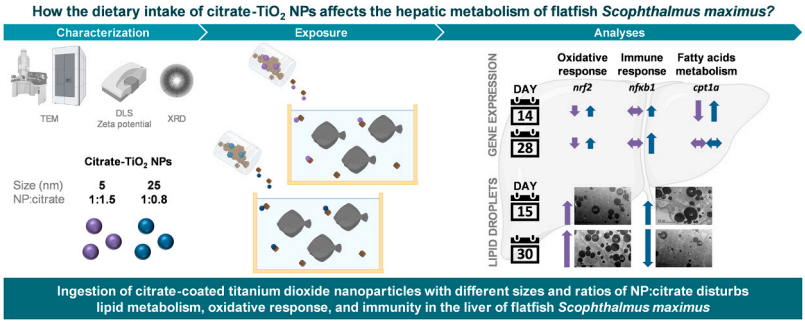


## ARTICLE INFO

Editor: Lingxin Chen

*Keywords:*
Titanium dioxide nanoparticles
Lipid metabolism
Inflammation
Oxidative stress
Steatosis

## ABSTRACT

The extensive use of nanomaterials, including titanium dioxide nanoparticles ($TiO_2$ NPs), raises concerns about their persistence in ecosystems. Protecting aquatic ecosystems and ensuring healthy and safe aquaculture products requires the assessment of the potential impacts of NPs on organisms. Here, we study the effects of a sublethal concentration of citrate-coated $TiO_2$ NPs of two different primary sizes over time in flatfish turbot, *Scophthalmus maximus* (Linnaeus, 1758). Bioaccumulation, histology and gene expression were assessed in the liver to address morphophysiological responses to citrate-coated $TiO_2$ NPs. Our analyses demonstrated a variable abundance of lipid droplets (LDs) in hepatocytes dependent on $TiO_2$ NPs size, an increase in turbot exposed to smaller $TiO_2$ NPs and a depletion with larger $TiO_2$ NPs. The expression patterns of genes related to oxidative and

* Corresponding author.
*E-mail address:* fonseca.ess@gmail.com (E. Fonseca).

https://doi.org/10.1016/j.jhazmat.2023.131915
Received 28 March 2023; Received in revised form 12 June 2023; Accepted 21 June 2023
Available online 22 June 2023

immune responses and lipid metabolism (*nrf2*, *nfκb1*, and *cpt1a*) were dependent on the presence of $TiO_2$ NPs and time of exposure supporting the variance in hepatic LDs distribution over time with the different NPs. The citrate coating is proposed as the likely catalyst for such effects. Thus, our findings highlight the need to scrutinize the risks associated with exposure to NPs with distinct properties, such as primary size, coatings, and crystalline forms, in aquatic organisms.

## 1. Introduction

Engineered nanoparticles (NPs) are becoming ubiquitous in our daily lives as a result of their widespread use in several applications, such as healthcare, industry and domestic household products. Because wastewater treatment effectiveness still varies significantly resulting in the incomplete removal of all incoming NPs, many of these NPs are transferred to and remain in aquatic ecosystems [147]. A variety of conditions, including media characteristics and biomolecule affinity, influence how dynamically NPs interact with biomolecules to form complexes. According to some authors, these compounds can be internalized and thus impact aquatic organisms at the biomolecular and cellular levels, causing morphological abnormalities in tissues (tissue ulceration, edema, gill irritation), differential expression of genes, and altering the activity of several enzymes (superoxide dismutase, catalase, acetylcholinesterase) [7,136].

Assessing the threat of NPs in aquatic organisms, such as non-model organisms and species of commercial interest, is becoming increasingly important since they are a new class of emerging contaminants with potential ecotoxicological impacts on aquatic ecosystems due to bioaccumulation, biotransformation, and biomagnification mechanisms [136]. Most data in this field comes from toxicity studies mainly undertaken for short-term exposure periods in model organisms of no commercial interest [73].

Among the numerous NPs currently produced, titanium dioxide ($TiO_2$) NPs are emerging for their broad range of applications, including biomedical and healthcare (e.g. drug delivery, sensors/probes, antimicrobials, tissue engineering), industrial and agricultural (e.g.: component in p-n heterojunction for solar energy conversion, pigments, preservatives), and domestic products such as personal care products (PCPs) (e.g. creams, sunscreens/ultraviolet radiation blockers, toothpaste) [1,3,5,46,51,98,99]. Titanium and titania are relevant for biomedical applications based on their low biological interaction (e.g.: prosthodontics and orthopaedics for dental and medical implants). Indeed, titania microparticles are considered less toxic than NPs, independently of the means of exposure [89]. Millions of tons of $TiO_2$ NPs are produced per year from inexpensive and highly abundant titanium minerals [77]. As a result of their use in PCPs, high concentrations of these NPs and their core elements have been found in sediment slides to wastewater outlets, as well as near popular tourist areas, such as the Mediterranean beaches [124,13,130,49]. In addition to waterborne and trophic exposure, cutaneous contact with NPs can make benthic aquatic species, including flatfish, more vulnerable to exposure than pelagic organisms [122,142]. Aquaculture species may potentially be exposed to NPs via water filtering/purification devices, feed additives, and other sources [73].

In line with research found in the literature [119,143,25,39,91], our previous work reported bioaccumulation of titanium in turbot liver after feeding exposure to $TiO_2$ NPs with a primary size of 25 nm and the resultant alterations in the proteins related to energy and lipid metabolism [10]. Nevertheless, there is still a paucity of knowledge on how exposure conditions affect the molecular pathways associated with $TiO_2$ NPs exposure in fish. In particular, the exposure duration, the average size within the nanometre range, the coating and functionalization strategy, and the structural and surface properties of NPs are highlighted among the parameters that can affect NPs toxicity (e.g.: [11,29,32,59,71,72,111,120]). In fact, studies considering simultaneously more than one NPs size, the contribution of coating and the effect of exposure on the expression of genes involved in different biological processes over time have been neglected.

Therefore, this work aims to study the histological and molecular effects induced by the ingestion of $TiO_2$ NPs with two different primary sizes in the liver of one Southern European Atlantic saltwater flatfish species of commercial and aquaculture interest, the turbot, *Scophthalmus maximus* (Linnaeus, 1758). In order to comprehend the impact of two $TiO_2$ NPs with the primary size of 5 and 25 nm, liver status was analysed at the cellular level. Bioaccumulation (determination of total titanium and $TiO_2$ NPs levels in the liver and faeces), hepatic histology, and relative expression of genes related to oxidative stress and inflammation and immune responses, endocrine system, and lipid metabolism were studied at two-time points after continuous exposure through the supply of contaminated feed.

## 2. Materials and Methods

### 2.1. Nanoparticles characterization

$TiO_2$ NPs powder used in this work was supplied by Nanostructured & Amorphous Materials, Inc. (Katy, TX, USA; code 5421ZH, anatase, 99%, 5 nm) and Sigma-Aldrich (Merk Life science, code 718467; 99.5% purity, mixture of rutile and anatase, 99.5%, 25 nm). The stock solutions of NPs were prepared as reported previously [10]. The weight ratio of $TiO_2$ NP:trisodium citrate dihydrate ($HOC(COONa)(CH_2COONa)_2$ 2 $H_2O$) was 1:1.5 for 5 nm $TiO_2$ NPs and 1:0.83 for 25 nm $TiO_2$ NPs. Briefly, the mixture of trisodium citrate dihydrate and $TiO_2$ NPs was dispersed in ultrapure water and artificial seawater to reach a concentration of 15 g/L and subsequently sonicated using an ultrasonic probe at 50% amplitude and cycles of 30 s pulse on/15 s pulse off for 30 min. The final dispersion was stored at 4 ºC until further use.

Dispersed $TiO_2$ NPs were characterized by X-Ray diffraction (XRD), Raman spectroscopy, transmission electron microscopy (TEM), dynamic light scattering (DLS) and zeta potential. XRD characterization was performed using a X'Pert PRO diffractometer (Malver Panalytical, Lisboa, Portugal) at 45 KV and 40 mA with a PIXcel detector and Cu Kα radiation ($\lambda = 1.541874$ Å). The data for phase composition identification were acquired using the Bragg-Brentano configuration in the 2θ range from 20 to 70 º with a scan speed of 0.01 °/s and a time per step of 298 s. The crystalline size was calculated using the Scherrer equation ($D=(k\lambda/\beta\cos\theta)$) where D is the crystalline size, k is Scherer's constant ($k = 0.94$), λ is the X-ray wavelength, β is the full width at half maximum (FWHM) of the XRD peak and θ is the Bragg angle [60]. The crystal phase was also analysed by Raman spectroscopy using an Alpha 300 R Witec miniconfocal Raman microscope (300 line $mm^{-1}$ grating and a CCD camera). Raman spectra were acquired for 5 s and 20 accumulations using a 785 nm excitation laser line and a 50x objective. TEM images were acquired using JEOL 2100 TEM operating at 200 kV (Izasa Scientific, Carnaxide, Portugal) for 25 nm $TiO_2$ NPs and FEI Titan Cubed Themis 60–300 kV operating at 200 kV (Thermo Fisher Scientific, Portugal) for 5 nm $TiO_2$ NPs. The samples for TEM analysis were prepared by dropping 5 μL of 20 mg/L of NPs dispersion on a carbon-coated 400 mesh copper grid and dried at room temperature. DLS and zeta potential analyses were performed using a SZ-100 device (Horiba, ABX SAS, Amadora, Portugal) to estimate the hydrodynamic size and surface charge, respectively, of $TiO_2$ NPs dispersed in both ultrapure water and artificial seawater at a concentration of 50 mg/L.

### 2.2. Biological material and experimental design

Two independent experimental trials were performed to study two citrate-coated $TiO_2$ NPs with primary sizes of 5 nm and 25 nm. These trials were carried out at the facilities of the Centro Tecnológico del Cluster de la Acuicultura (CETGA, Spain). Juvenile turbots (*Scophthalmus maximus*) were allowed to acclimate for one week before each trial. During the trials, turbots were kept in open flow systems composed of 1 $m^3$ indoor tanks (50 fish per tank at the beginning of the trials, three tanks per treatment group) with constantly running pre-filtered seawater (50 μm), 35‰ salinity and a photoperiod of 14 h:10 h (light: dark). In the 5 nm $TiO_2$ NPs trial, the mean water temperature was 14.0 ± 1.2 °C and the initial average weight of fish was 73.0 ± 0.5 g. with a daily feeding rate of 1.5% and 1.1% of their body weight (Table 3). In the 25 nm $TiO_2$ NPs trial, the mean water temperature was 13.6 ± 1.2 °C and the initial average weight of fish was 45.0 ± 1.0 g with a daily feeding rate of 2% and 1.5% of their body weight (Table 3). All fish were fed four times per day by hand and feeds were fortnightly adjusted within all treatments during the experiments. Observations of fish death, health and behaviour were performed daily. $TiO_2$ NPs were incorporated in commercial pellets (Biomar Iberia, S.A.) previously coated with micronized calcium carbonate (5% $CaCO_3$, C.T.S. España S. L.). The concentrations of $TiO_2$ NPs were prepared to complete 0 or 1.5 mg of NPs per kg of fish per day for each NPs size.

The effects on growth were determined by evaluating weight gain (WG), specific growth rate (SGR) and food conversion ratio (FCR) according to the following formulas: *WG = final body weight - initial body weight*; *SGR = 100 × [ln (final body weight) - ln (initial body weight)]/n days*; *FCR = feed intake/weight gain*. Statistical analysis was performed to compare fish weights using Statgraphics Centurion XVI (Statpoint Technologies Inc., The Plains, VA). A one-way analysis of variance (ANOVA) was calculated to detect significant differences between control and treated groups at each sampling time, followed by Fisher's Least Significant Difference for multiple range test analysis ($\rho < 0.05$).

For further analyses, fish were weighed and killed by overexposure to MS-222 (Sigma-Aldrich) after 14, 15, 28, and 30 days. All experimental procedures were carried out under European Union and Spanish regulations [R.D. 53/2013 (BOE, 2013), and Council Directive 2010/63/EU (EU, 2010)] for the protection of animals used for experimental purposes by personnel qualified in animal experimentation in authorized facilities by competent Spanish authority (REGA ES150730055401).

### 2.3. Transmission electron microscopy imaging of turbot liver

Liver samples from two fish (each individual fish taken from two tanks per treatment group, n = 2) were collected on days 15 and 30 and fixed overnight at 4ºC using Karnovsky's fixative (2% paraformaldehyde, 2.5% glutaraldehyde, 0.1 M sodium cacodylate buffer) and stored at 4ºC under shaking until further use. Liver fragments were post-fixed in a 1% osmium tetroxide solution, dehydrated with increasing ethanol concentration (50–100%) and with a final emersion on propylene oxide. The infiltration was made in mixtures of propylene oxide:epoxy resin (EMBed-812 kit) at different proportions, increasing the amount of resin until 100% epoxy resin was achieved. The cure of the blocks was at 60 °C for three days.

Ultrathin sections (≈80 nm thick) were made in a PowerTome PC ultramicrotome (RMC Boeckeler, USA), with a diamond knife (Diatome) and placed on formvar/carbon 200 mesh copper grids. TEM micrographs of the sections were taken with a JEOL JEM 1010 transmission electron microscope (Izasa Scientific, Madrid, Spain) operating at 100 kV.

### 2.4. Determination of total titanium and $TiO_2$ NPs levels in turbot liver, and faeces

Liver samples from two fish (each individual fish taken from two tanks per treatment group, n = 2) were collected on days 15 and 30 and stored at -20 ºC. Faeces samples were collected from the bottom of tanks before and after feeding (separate pooled samples with at least 0.250 g). Total titanium and $TiO_2$ NPs levels were determined in turbot liver and faeces as previously stated in [10] and described in detail in the Supplementary Material. Briefly, total titanium was determined by Inductively Coupled Plasma-Mass Spectrometer (ICP-MS). Determination of $TiO_2$ NPs in the liver was also performed by the ICP-MS in single-particle mode. $TiO_2$ NPs could not be determined in faecal samples due to limited sample availability.

### 2.5. Relative gene expression

Liver samples were collected on days 14 and 28 (pools of three fish per tank from each treatment group, n = 3) and stored in RNAlater (Sigma-Aldrich) at -20 ºC until further use. The total RNA of liver samples was extracted and purified using RNeasy Mini Kit (Qiagen) with a step of on-column DNaseI digestion and eluted with RNase-free water. The quantification and integrity of RNA were assessed by spectrophotometry (Denovix) and electrophoresis (2% agarose gel). The First-strand cDNA Synthesis Kit (NZYTech) was used following the manufacturer's recommendations to synthesize cDNA from 2500 ng of the total RNA previously purified.

The nucleotide sequences of the selected genes (*nrf2*, *nfκb1*, *gr1*, *thrαb*, *pparαb*, *lxrα*, *fasn*, *elovl5*, *cpt1a*, *acox1* and *hadh*) and reference genes (*18 s* and *ef1α*) were recovered from GenBank [19]. Primers for reference genes were based on a previous study [38] and the remaining primers were designed manually out-flanking one intron to obtain products around 112–242 bp (Table 1). Primers' specificity was tested with a gradient polymerase chain reaction (PCR) and confirmed by visualization of the PCR products in a 2% agarose gel.

Quantitative PCR (qPCR) was performed to analyse the expression levels of genes related to oxidative stress, immunologic response, endocrine system regulation, and lipid metabolism, using PowerUp SYBR Green PCR Master Mix (Applied Biosystems) on Step One Plus Real-Time PCR system (Applied Biosystems). Liver cDNA samples were amplified in triplicates or duplicates, with 5 μL of PowerUp SYBR Green PCR Master Mix (2x), 0.5 μL of each primer at 10 μM, 2 μL of cDNA at 50 ng and RNase-free water was added to a reaction volume of 10 μL. A two-step reverse-transcription PCR program was performed: UDG activation at 50 °C for 2 min and DNA polymerase activation at 95 °C for 2 min, followed by 40 cycles of denaturation at 95 °C for 3 s and combined annealing and extension between 58 °C and 60 °C for 30 s (Table 1). At the end of each run, a dissociation step was performed to generate a melting curve to confirm the specificity of the reactions. Serial dilutions of a cDNA pool with all samples (15.6–500 ng) were used to produce standard curves and calculate the efficiency of each pair of primers (Table 1). Changes in target gene expression levels were estimated for two housekeeping genes (*18s* and *ef1α*) and normalized to control groups (0.0 mg/Kg) using the Pfaffl method [109]. The means of the fold-change in relative gene expression and the bars with standard error of the mean (SEM) from the three pools were computed for graphical representation. The statistical analysis was performed with R-Studio v2022.07.2. A two-way factorial analysis of variance (ANOVA) was calculated for each independent assay to compare the differences between the gene expression average of groups treated for 14 or 28 days with $TiO_2$ NPs (1.5 mg/Kg), followed by pairwise multiple comparisons with the Bonferroni correction. The statistical assumptions for all factorial ANOVAs have been met, including homogeneity of variances (Levene's test with ρ-value > 0.05) and residuals normally distributed (Shapiro test with ρ-value > 0.05), except ANOVAs for genes *lxrα* (5 nm $TiO_2$ NPs trial) and *thrαb* (25 nm $TiO_2$ NPs trial), for which residuals were not normally distributed. However, the variables for these two genes were not transformed, as ANOVA is commonly robust to violations of normality [22,116]. The differences with a ρ-value less than 0.05 were considered statistically significant.

**Table 1**
Sequences of primer used for qPCR analyses and PCR efficiency.

| Gene acronym | Gene name | Endpoint | Accession number | Sequence 5' → 3' | Tm (°C), Product size (bp), Average efficiency (%) |
|---|---|---|---|---|---|
| *nrf2* | nuclear factor erythroid 2–related factor 2 | Antioxidant response | AWP13156.1 | F: CTCGACGAGGAGACGGGA<br>R: ATCATGTTGCCGCTGCTGG | 60, 242, 95 |
| *nfκb1* | nuclear factor kappa b subunit 1 | Inflammation, immunity | AWP11578.1 | F: AGGAAGACCTACCCCACC<br>R: ACCAGACTGTGAGCGTGAAG | 60, 113, 98 |
| *gr1* | glucocorticoid receptor 1 | Hormone signalling, inflammation | AWP12225.1 | F: GTGTCCAAACTGTGTCTCC<br>R: AGCCTCGTCCGAACACAC | 60, 231, 98 |
| *Thrαb* | thyroid hormone receptor alpha b | Hormone signalling | AWP18067.1 | F: CGCCATCTTCGACCTGGG<br>R: AAGTGGGGAACGTTGTGC | 58, 194, 127 |
| *pparαb* | peroxisome proliferator-activated receptor alpha b | Lipid metabolism, inflammation | JX975469.1 | F: CTCGAACCATTCTCACCG<br>R: CCACCGATGTGCACTGGC | 60, 174, 101 |
| *Lxrα* | liver x receptor alpha | Lipid homeostasis, inflammation | AWP01219.1 | F: GGCTTCAGTTTGAGTTCATCAAC<br>R: TCATGATGTAGGAGCGCAGC | 60, 195, 105 |
| *Fasn* | fatty acid synthase | Lipid metabolism (biosynthesis) | AWP17114.1 | F: GGCAACAACACGGATGGATAC<br>R: CTCGCTTTGATTGACAGAACAC | 60, 205, 97 |
| *elovl5* | elongation of very long chain fatty acids 5 | Lipid metabolism (biosynthesis) | AF465520.2 | F: CCTACTATGGCCTGTCAGC<br>R: AAAGGATAATCAGCGTGACCAC | 60, 192, 109 |
| *cpt1a* | carnitine palmitoyltransferase 1 a | Lipid metabolism (β-oxidation) | XP_035499111.2 | F: CTGAGCCATGGAGACTGTC<br>R: AGTGTTTGCTGGAGATGTGG | 60, 186, 115 |
| *acox1* | acyl-CoA oxidase 1 | Lipid metabolism (β-oxidation) | AWP05881.1 | F: CGTGTCATACCTGAGTGAAGC<br>R: GGTCGATAGCACTGTTGTTCC | 60, 215, 104 |
| *Hadh* | hydroxyacyl-CoA dehydrogenase | Lipid metabolism (β-oxidation) | AWP05488.1 | F: CATTGTGAACCGCCTGCTTG<br>R: GTCTAGTCCCACATAGTCCG | 60, 154, 106 |
| *18s* | 18S rRNA | Housekeeping gene | EF126038.1 | F: CTCAACACGGGAAACCTCAC<br>R: ATCGCTCCACCAACTAAGAAC | 60, 112, 96 |
| *ef1α* | eukaryotic translation elongation factor 1 alpha 1 | Housekeeping gene | AF467776.1 | F: TATTAACATCGTGGTCATTGG<br>R: CAGGCGTACTTGAAGGAG | 60, 153, 97 |

## 3. Results

### 3.1. Characterization of nanoparticles

$TiO_2$ NPs were characterized by XRD, Raman spectroscopy, TEM, DLS and zeta potential. The crystalline phase analysis of 5 nm $TiO_2$ NPs displayed an XRD pattern with diffraction peaks related to the anatase phase (Fig. 1**A** purple spectrum), as stated by the supplier. The bicrystalline structure expected for 25 nm $TiO_2$ NPs, which are typically composed of 80% anatase and 20% rutile, was confirmed by the XRD pattern with peaks corresponding to anatase and rutile crystalline phase and a majority of NPs with single anatase or rutile phases (Fig. 1**A** green spectrum) [66]. The diffraction peaks are broader for 5 nm $TiO_2$ NPs than for 25 nm $TiO_2$ NPs due to the NP size effect on the XRD pattern. The broadness increment is more pronounced for sizes smaller than 10 nm [14]. This size dependence offers the possibility to estimate the size of NP crystallite with XRD spectra by applying the Scherrer equation. Hence, we obtained Scherrer's crystallite sizes of 8.6 nm for the anatase phase in 5 nm $TiO_2$ NPs, whereas in 25 nm $TiO_2$ NPs, we calculated sizes of 18.1 nm and 23.9 nm for the anatase and rutile phases, respectively. Larger crystallite sizes for the rutile phase than for the anatase phase were previously reported [18] and were consistent with the size distribution of 29 ± 10 nm estimated by TEM [10].

In concordance with the XRD results, the anatase phases were also detected in the Raman spectra (Fig. 1**B**). The $E_g$ mode centred at 145–151, 197, and 640 $cm^{-1}$ represent the symmetric stretching vibration of O-Ti-O in $TiO_2$. Similarly, the $B_{1\,g}$ mode centred at 399 $cm^{-1}$ and the $A_{1\,g}$ mode centred at 519 $cm^{-1}$ correspond to the symmetric and antisymmetric bending vibration of O-Ti-O, respectively. Furthermore, a weak peak centred at 455 $cm^{-1}$ is assigned to the $E_g$ mode of the rutile phase in 25 nm $TiO_2$ NPs (Fig. 1**B**, green spectrum). The relatively low intensity of this peak is attributed to the fact that the rutile crystalline phase constitutes only a minor fraction (≤ 20%) of the overall composition of 25 nm $TiO_2$ NPs. Additionally, in the Raman spectrum of 5 nm $TiO_2$ NPs (Fig. 1**B**, purple spectrum), the $E_g$ peak of anatase exhibited a redshift centred at 151 $cm^{-1}$ and a broader profile, with a Full Width at Half Maximum (FWHM) of 47.6 $cm^{-1}$ in comparison with the corresponding peak for 25 nm $TiO_2$ NPs which appeared at 145 $cm^{-1}$ with a narrower FWHM of 13 $cm^{-1}$. These differences can be attributed to the size effect, wherein larger redshifts and broadening occur as the size of $TiO_2$ NPs decreases, as previously reported [31].

The shape and primary size distribution of $TiO_2$ NPs were determined using TEM. This analysis showed that most $TiO_2$ NPs have an elliptical shape and form aggregates (Fig. 1**C-F**). However, 25 nm $TiO_2$ NPs exhibited some anisotropic NPs, such as cubes (Fig. 1**E-F**). The primary size of 5 nm $TiO_2$ NPs could not be accurately calculated due to the overlap of primary NPs (Fig. 1**D-F**) even by employing an aberration-corrected TEM, which offers atomic resolution [80]. Despite the challenge of clearly identifying the boundaries of many single particles, the size distribution of these NPs was estimated to be under 10 nm.

The colloidal stability of 50 mg/L $TiO_2$ NPs in ultrapure water and artificial seawater was characterized by DLS and zeta potential to assess the behaviour of the NPs that may be released from the pellets during the feeding. In ultrapure water, the hydrodynamic size of both 5 nm and 25 nm $TiO_2$ NPs (53 nm and 166 nm, respectively) was higher than the size estimated by TEM and XRD, confirming the formation of aggregates (Table 2). The polydispersity index (PDI) suggested a more homogeneous size distribution for 25 nm $TiO_2$ NPs compared to 5 nm $TiO_2$ NPs, and the zeta potential values indicated that both NPs had a negative surface charge (Table 2). In contrast, larger hydrodynamic sizes and PDIs were observed for both NPs in artificial seawater, suggesting the formation of larger and more heterogeneous aggregates compared to ultrapure water (Table 2). This behaviour can be attributed to the destabilizing effect of the high concentration of salts in seawater, aligning with the zeta-potential values close to zero [96].

### 3.2. Mortality, feeding, and fish behaviour

No external injuries or mortality were recorded in fish during the tests, and no behavioural alterations were observed in fish exposed to 5 nm $TiO_2$ NPs (Table 3). Food leftovers were observed in the 25 nm $TiO_2$ NPs treatment tanks, while all the food was consumed in the control tanks. On day 14, a decrease in weight gain was registered in the $TiO_2$ NPs treated group compared to the control group (Table 3). The properties of $TiO_2$ as a food additive may alter food palatability and fish appetite [97,138]. From day 14 onward, the daily feeding rate was

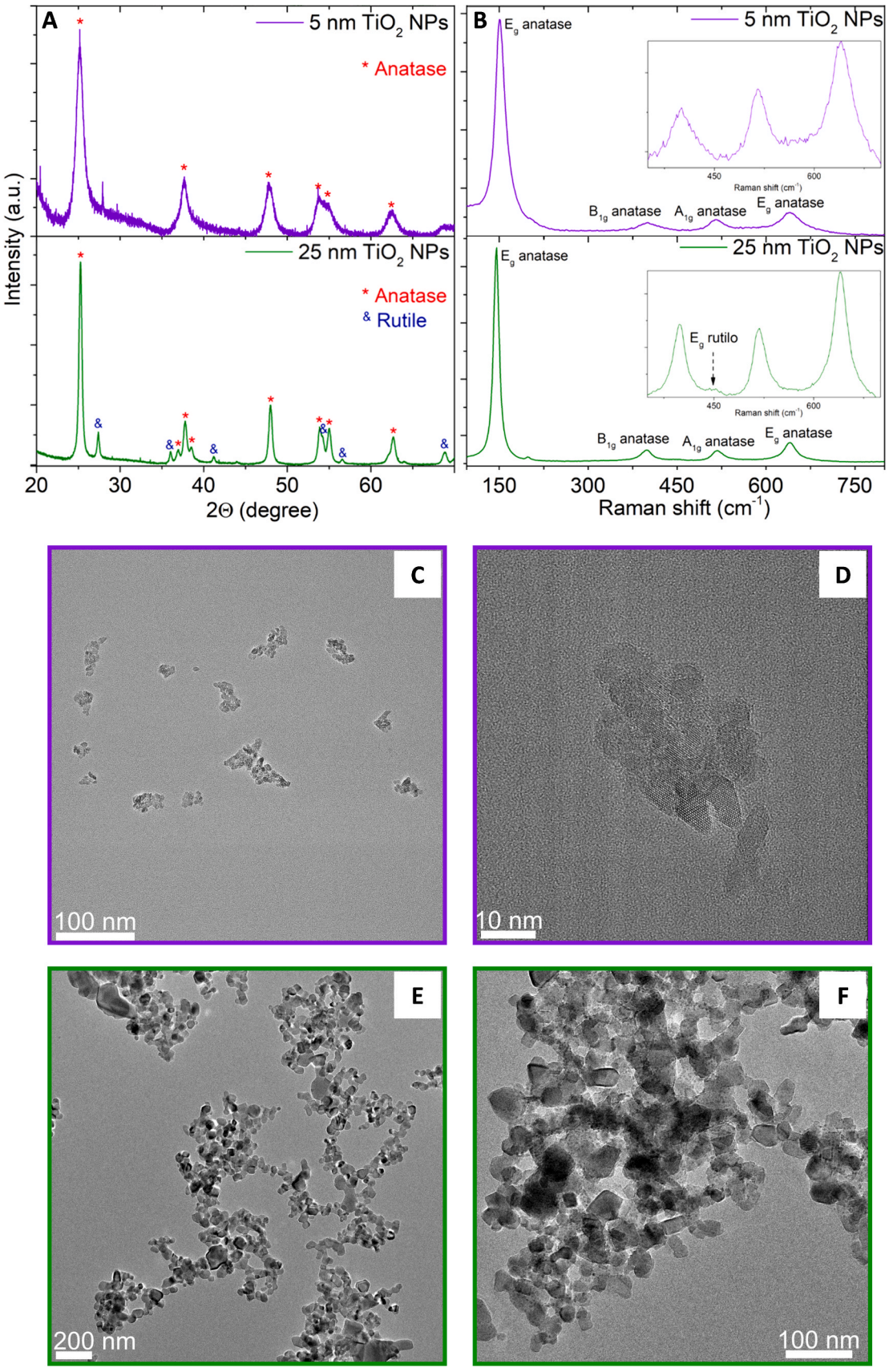


**Fig. 1.** Physicochemical characterizations of citrate-coated $TiO_2$ NPs. Crystalline phase characterization by XRD (A) and Raman spectroscopy (B) and TEM images of 5 nm (C, D) and 25 nm (E, F) $TiO_2$ NP aggregates. The identified crystalline phases are indicated by * for anatase and & for rutile; XDR and Raman spectra of 5 nm and 25 nm $TiO_2$ NPs are represented in purple and green, respectively. $TiO_2$ NPs were placed on glass slides upon excitation at 785 nm. The inset in each Raman spectra indicates zooming in the spectral window from 350 to 700 $cm^{-1}$.

**Table 2**
Physicochemical characterization of selected $TiO_2$ NPs before exposure by DLS (n = 5) and zeta potential (n = 5).

| | 5 nm $TiO_2$ NPs | | 25 nm $TiO_2$ NPs | |
|---|---|---|---|---|
| | Ultrapure water | Artificial seawater | Ultrapure water | Artificial seawater |
| Hydrodynamic diameter[a] (nm) | 53 ± 2 | 6969 ± 408 | 166 ± 3 | 7589 ± 2291 |
| Polydispersity index[b] | 0.47 ± 0.06 | 5.13 ± 0.53 | 0.19 ± 0.03 | 2.11 ± 0.99 |
| Z potential[c] (mV) | - 61 ± 14 | - 2 ± 3 | - 79 ± 2 | - 2 ± 1 |

[a] Mean hydrodynamic diameter.
[b] polydispersity index obtained by DLS at a scattering angle of 173° and 25 °C. Five DLS measurements were acquired: mean ± standard deviation (SD).
[c] Zeta potentials were measured in 5 runs (mean ± SD).

**Table 3**
Fish's weight and feeding features on the 5 nm and 25 nm $TiO_2$ NPs trials. The values with * are statistically significant (ρ-value < 0.05).

| 5 nm $TiO_2$ NPs trial | | | | |
|---|---|---|---|---|
| Period time (day) | 0–14 | | 14–28 | |
| Daily feeding rate (%) | 1.5 | | 1.1 | |
| NPs dose (mg/Kg) | 0.0 | 1.5 | 0.0 | 1.5 |
| Initial weight (g) ± SD | 72.7 ± 0.2 | 73.3 ± 1.0 | 97.9 ± 2.4 | 96.1 ± 2.2 |
| Average weight (g) ± SD | 97.9 ± 2.4 | 96.1 ± 2.2 | 115.7 ± 5.2 | 118.5 ± 5.9 |
| Weight gain (g) ± SD | 25.2 ± 0.6 | 22.8 ± 0.5 | 17.8 ± 0.8 | 22.4 ± 1.1 |
| Specific growth rate (%) ± SD | 2.1 ± 0.1 | 1.9 ± 0.0 | 1.2 ± 0.1 | 1.5 ± 0.1 |
| Feed conversion rate (%) ± SD | 0.6 ± 0.02 | 0.7 ± 0.02 | 0.8 ± 0.04 | 0.7 ± 0.03 |
| 25 nm $TiO_2$ NPs trial | | | | |
| Period time (day) | 0–14 | | 14–28 | |
| Daily feeding rate (%) | 2.0 | | 1.5 | |
| NPs dose (mg/Kg) | 0.0 | 1.5 | 0 | 1.5 |
| Initial weight ± SD | 45.0 ± 1.0 | 45.0 ± 1.1 | 66.6 ± 9.5 * | 55.8 ± 6.0 * |
| Average weight (g) ± SD | 66.6 ± 9.5 * | 55.8 ± 6.0 * | 86.0 ± 15.4 | 79.5 ± 12.7 |
| Weight gain (g) ± SD | 21.6 ± 3.1 | 10.8 ± 1.2 | 19.4 ± 3.5 | 23.7 ± 3.8 |
| Specific growth rate (%) ± SD | 2.61 ± 0.4 | 1.44 ± 0.2 | 1.96 ± 0.4 | 2.72 ± 0.4 |
| Feed conversion rate (%) ± SD | 0.6 ± 0.09 | 1.2 ± 0.13 | 0.7 ± 0.12 | 0.5 ± 0.07 |

reduced from 2% to 1.5%, and no leftovers were observed in any of the tanks. At the end of the trial, no significant changes were observed in fish weight (Table 3), possibly due to fish adaptation to organoleptic characteristics of the NP-containing diet or adjustment in the daily feeding rate. The differences observed between the two trials may be attributed to an insufficient concentration of NPs [84] or variations in NPs size and $TiO_2$ NPs:citrate ratio. Moreover, the absence of mortality is consistent with previous results [42,93] and supports the view that fish are less sensitive to $TiO_2$ NPs than other marine organisms, such as cladocerans or algae in chronic toxicity tests [53].

### 3.3. Detection of titanium in the liver and faeces

Total titanium and $TiO_2$ NPs levels were determined in the liver and faeces of turbots after 15 and 30 days of exposure to 5 nm and 25 nm $TiO_2$ NPs (Supplementary Table S1). No traces of $TiO_2$ NPs were found in the liver (Limit of Detection, $LOD_{number} = 2.52 \times 10^4$ NPs $g^{-1}$, $LOD_{size}$ = 42 nm), and the limited amount of faecal samples hindered the determination of $TiO_2$ NPs. In general, titanium was detected in the control and exposed fish, and the highest levels of titanium were measured in the 5 nm $TiO_2$ NPs trial. Furthermore, higher concentrations of titanium were detected in the liver of fish exposed to both $TiO_2$ NPs after 15 days compared to 30 days (Supplementary Table S2). Nevertheless, the accumulation of titanium was higher in fish exposed to 25 nm $TiO_2$ NPs than in fish exposed to 5 nm $TiO_2$ NPs. Additionally, the faecal titanium levels of fish exposed to 5 nm and 25 nm $TiO_2$ NPs were approximately 13- and 7-fold greater, respectively, than in the faeces of the control fish (Supplementary Table S2). These results indicated that $TiO_2$ NPs and titanium have a low potential to bioaccumulate in the liver of turbots, being excreted in the faeces.

### 3.4. Cellular ultrastructure

No $TiO_2$ NPs, nor any significant disruption in the ultrastructure of the tissues or cells, were observed in any of the conditions. However, as can be observed in Fig. 2, control hepatocytes contain several lipid droplets (LDs). These LDs seem to be slightly higher in size and number over time, which is expected as turbot juveniles are growing and rapidly gaining weight (control group). However, when exposed to $TiO_2$ NPs through feed intake, larger LDs, reaching the size of giant LDs (> 10 μm), were observed [48]. In our previous work, we postulated that the observation of larger but fewer LDs when fish were exposed to 25 nm $TiO_2$ NPs during 14 days could be due to the process of LDs coalescence perhaps due to insufficient phosphatidylcholine to cover the LD surface and lower surface tension to maintain a metastable state or to accumulate fatty acids derived from oxidative stress [10]. After 30 days of exposure, the trend seems to change, with smaller LDs observed in the hepatocytes. However, in the case of the 5 nm $TiO_2$ NPs, the size of LDs tends to increase over time without an apparent decrease in number.

### 3.5. Relative gene expression

The effects of exposure to different sizes of $TiO_2$ NPs were studied in terms of lipid metabolism, hormone signalling (endocrine system), immunity, inflammation, and oxidative stress (Table 1) through alterations in the expression of a set of 11 genes in two periods of time (14 and 28 days) (Fig. 3).

The exposure of juvenile turbots to 5 nm $TiO_2$ NPs led to a significant change in the expression of *cpt1a* in the liver after 28 days of exposure (ρ = 0.026; Table 4), an effect dependent on the dose of $TiO_2$ NPs (ρ = 0.028; Table 4). The difference in the expression of *cpt1a* was confirmed in the follow-up analysis using the Bonferroni correction (ρ = 0.031; Fig. 3**A**). Additionally, we have found some potential changes in gene expression, although these changes were not statistically significant (ρ > 0.05, Table 4 and Fig. 3**A**). The expression of *gr1*, *pparαb*, and *lxrα* tendentially increased after 28 days of exposure as well as *hadh* after 14 and 28 days of exposure to 5 nm $TiO_2$ NPs. There was also a tendency for a decrease in the expression of *nrf2*, *thrαb*, and *elovl5* in the 5 nm $TiO_2$ NPs exposed group. No significant changes in gene expression levels were detected for the remaining genes included in our study (ρ > 0.05, Table 4 and Fig. 3**A**).

The treatment of juvenile turbots with 25 nm $TiO_2$ NPs also led to a significant alteration in *cpt1a* expression affected by the dose of NPs and the time of exposure (ρ = 0.029 and ρ = 0.018, respectively, Table 4). However, the effects of exposure time do not seem to be dependent on the ingestion of 25 nm $TiO_2$ NPs (ρ = 0.056, Table 4). The Bonferroni correction confirmed the increased expression of *cpt1a* in the livers after 14 days of exposure to 25 nm $TiO_2$ NPs compared to the control group (ρ = 0.038, Fig. 3**B**). The ingestion of 25 nm $TiO_2$ NPs and the treatment duration significantly affected the expression of *nfκb1* (ρ < 0.001 and ρ = 0.046, respectively, Table 4) with a significant dependence between the dose and the time of exposure (ρ = 0.038, Table 4). The follow-up analysis supported the significant increase of *nfκb1* after 28 days of exposure to 25 nm $TiO_2$ NPs (ρ = 0.002, Fig. 3**B**). Both *nrf2* and *acox1* expression levels were affected by the presence of 25 nm $TiO_2$ NPs (ρ < 0.039 and ρ < 0.022, respectively, Table 4) despite the significant differences among groups not being corroborated by the Bonferroni correction (ρ > 0.05). Among the genes with no significant differences in their expression levels (ρ < 0.05, Table 4 and Fig. 3**B**), *thrαb* and *gr1* tended to increase after 14 days of treatment. As was observed in the 5 nm $TiO_2$ NP treatments, the expression of *hadh* slightly increased when turbots were treated with 25 nm $TiO_2$ NPs, contrasting with the

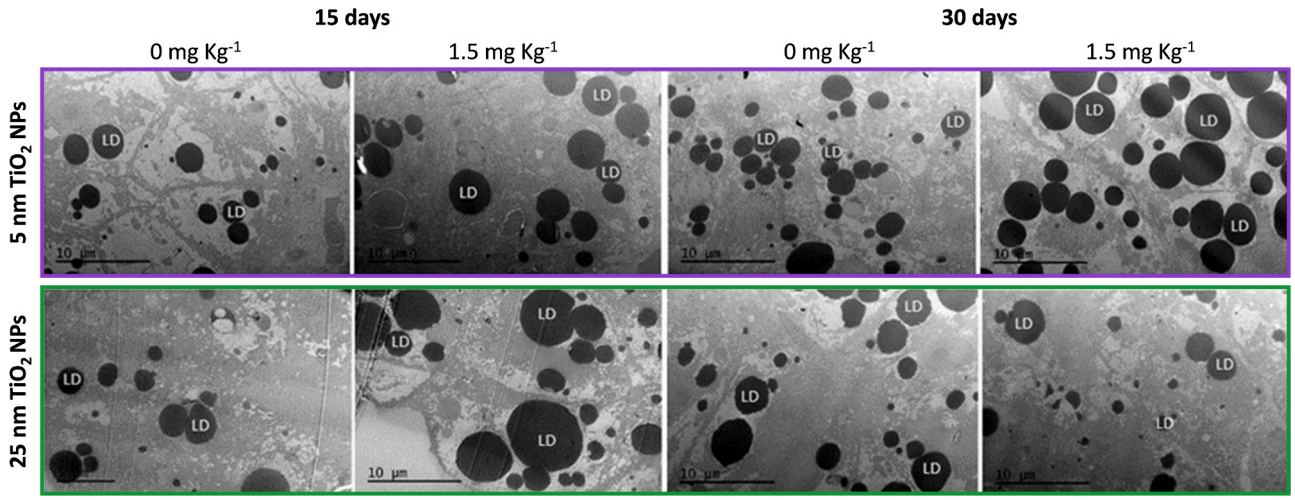


**Fig. 2.** Transmission electron microscopy images of liver sections from control and exposed turbots (n = 2) showing hepatocytes filled with lipid droplets (LDs).

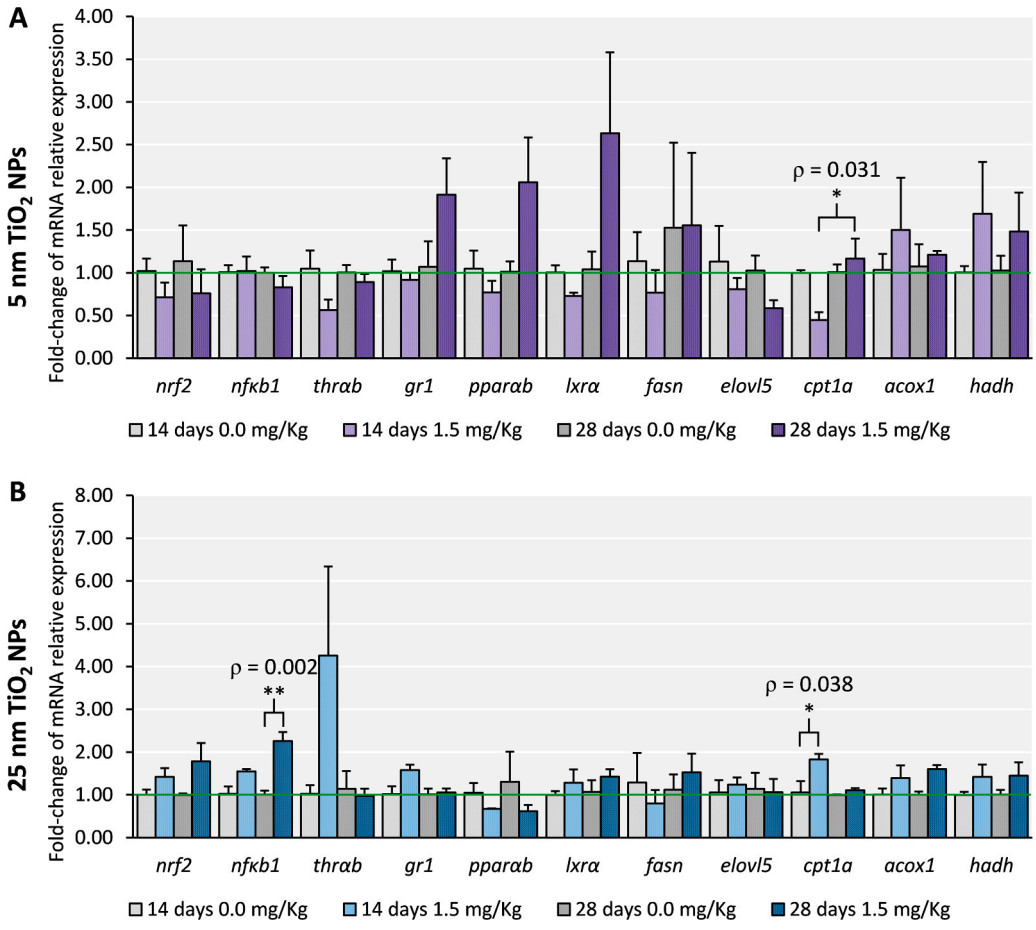


**Fig. 3.** Effects of exposure to citrate-coated $TiO_2$ NPs on expression levels of genes related to oxidative stress response, inflammation, endocrine system, and lipid metabolism in the liver of juvenile turbots. Statistically significant changes in gene expression (n = 3) were confirmed with the Bonferroni correlation (* $\rho < 0.05$; ** $\rho < 0.01$).

decreased expression of *pparαb*.

## 4. Discussion

The toxicity of $TiO_2$ is controversial since it has been considered "biologically" inert [54] and has been widely used as a food additive (E171) to enhance the flavour, whiteness, and brightness of a variety of food products [108]. However, recent studies have drawn attention to the hazardous effects of nanomaterials, including $TiO_2$ NPs, on a wide variety of organisms, such as soil microbes, human gut microbiota, fish, molluscs, crustaceans [79,84,86,123]. Consequently, there are increasing concerns regarding the potential risks associated with human consumption [15,21,45,62,8].

Currently, several mechanisms involved in the cytotoxicity of

**Table 4**
Statistical significance of $TiO_2$ NPs on relative gene expression: dependence on the presence of NPs and duration of the exposure for each NPs. Two-way ANOVA followed by Bonferroni correction; statistically significant values (ρ-value < 0.05) are shown in bold.

| | | 5 nm $TiO_2$ NPs | | 25 nm $TiO_2$ NPs | |
|---|---|---|---|---|---|
| Genes | Factors | $F_{(1,8)}$ | ρ-value | $F_{(1,8)}$ | ρ-value |
| *nrf2* | Time | 0.086 | 0.777 | 0.525 | 0.489 |
| | Dose | 1.527 | 0.252 | **6.045** | **0.039** |
| | Time x Dose | 0.016 | 0.903 | 0.554 | 0.478 |
| *nfκb1* | Time | 0.658 | 0.441 | **5.567** | **0.046** |
| | Dose | 0.439 | 0.526 | **36.613** | **< 0.001** |
| | Time x Dose | 0.601 | 0.461 | **6.137** | **0.038** |
| *thrαb* | Time | 1.052 | 0.335 | 2.182 | 0.178 |
| | Dose | 4.711 | 0.062 | 2.053 | 0.190 |
| | Time x Dose | 1.799 | 0.217 | 2.511 | 0.152 |
| *gr1* | Time | 3.732 | 0.089 | 3.729 | 0.090 |
| | Dose | 1.852 | 0.211 | 4.897 | 0.058 |
| | Time x Dose | 3.019 | 0.120 | 3.558 | 0.096 |
| *pparαb* | Time | 4.455 | 0.068 | 0.076 | 0.790 |
| | Dose | 1.671 | 0.232 | 1.983 | 0.197 |
| | Time x Dose | 4.989 | 0.056 | 0.181 | 0.682 |
| *lxrα* | Time | 3.952 | 0.082 | 0.220 | 0.652 |
| | Dose | 1.819 | 0.214 | 2.001 | 0.195 |
| | Time x Dose | 3.673 | 0.092 | 0.028 | 0.872 |
| *fasn* | Time | 0.735 | 0.416 | 0.341 | 0.576 |
| | Dose | 0.062 | 0.810 | 0.007 | 0.937 |
| | Time x Dose | 0.083 | 0.781 | 0.914 | 0.367 |
| *elovl5* | Time | 0.465 | 0.515 | 0.024 | 0.881 |
| | Dose | 2.525 | 0.151 | 0.030 | 0.868 |
| | Time x Dose | 0.059 | 0.814 | 0.196 | 0.670 |
| *cpt1a* | Time | **7.410** | **0.026** | **7.042** | **0.029** |
| | Dose | 2.146 | 0.181 | **8.756** | **0.018** |
| | Time x Dose | **7.151** | **0.028** | 4.976 | 0.056 |
| *acox1* | Time | 0.134 | 0.724 | 0.340 | 0.576 |
| | Dose | 0.765 | 0.407 | **7.951** | **0.022** |
| | Time x Dose | 0.223 | 0.649 | 0.396 | 0.547 |
| *hadh* | Time | 0.056 | 0.818 | 0.009 | 0.928 |
| | Dose | 2.163 | 0.180 | 3.870 | 0.085 |
| | Time x Dose | 0.085 | 0.778 | 0.001 | 0.975 |

nanomaterials are known and summarised as follows:

1) Cell membrane damage by the direct physical interaction of sharp-edged nanomaterials with the cell wall membrane [4,33]. In the case of $TiO_2$ NPs, the anatase crystallite induces more damage due to its greater abrasiveness compared to rutile crystallite [2,141].
2) Limitation of cell mobility and impairment of cellular function (cell-cell communication, nutrient exchange, and waste removal) by trapping cells within aggregated nanomaterials [57,63]. $TiO_2$ NPs can peroxidize lipids in cell membranes and consequently enter and accumulate inside cells, leading to an increase in reactive oxygen species (ROS), alteration in the molecular pattern of several biomolecules, DNA damage and tubulin depolymerization [113].
3) ROS generation and oxidative stress since nanomaterials have high oxidative potential. The increased ROS production disrupts the cellular redox balance causing oxidative stress [2,148]. In fish, the excessive production of ROS induced by $TiO_2$ NPs exposure impairs hepatic antioxidant mechanisms and the endocrine system [127,41,55].
4) DNA damage and genotoxicity via oxidative stress induced by ROS production can lead to genetic mutations, chromosomal aberrations, and other genotoxic effects [112,135,76]. Genotoxicity is also dependent on the size and shape of nanomaterials, with smaller $TiO_2$ NPs and $TiO_2$ nanofibers causing more severe damage [118,6,81].
5) Formation and subsequent explosion of nanobubbles by decomposition of engineered nanocomposite containing $O_2$ in response to irradiation, and changes in pH or temperature. The generation and collapse of nanobubbles create strong mechanical forces able to cause physical damage to cells around the nanocomposite [64,65].
6) Release of metal ions into the environment or inside organisms induces oxidative stress, disrupts cellular functions, and interferes with various biochemical processes. $TiO_2$ NPs are considered insoluble and resistant to dissolution. However, the rapid ion release can produce short-term toxic effects similar to those of dissolved ions, while the slower ion release can cause long-term adverse effects [90].
7) Cell metabolism impairment by disrupting cellular processes, such as mitochondrial function, glycolysis, lipid metabolism, and proteins and RNA degradation pathways, leading to energetic imbalance and contributing to cell dysfunction or cell death [131]. Such effects also affect fish, contributing to thyroid endocrine disruption, changes in circadian rhythm and immune response [27,68,79].

In the current research, we assessed morphophysiological changes in the liver of turbot after ingestion of different-sized $TiO_2$ NPs with a citrate coating, relating the cellular uptake and accumulation of these NPs and the expression patterns of genes involved in oxidative stress and inflammation and immune responses, endocrine system, and lipid metabolism.

### *4.1. Accumulation of titanium in the liver and faeces*

The cellular mechanisms underlying the uptake of NPs are multifaceted and influenced by various physicochemical properties [16]. Briefly, NPs enter the cells mainly through endocytosis, a process more effective for 50 nm-sized NPs than smaller or larger NPs. Spherical NPs undergo higher cellular uptake than rod-shaped NPs. However, NPs with large surface area exhibit heightened internalization, which is believed to be a consequence of increasing the probability of locating and interacting with cellular receptors for uptake. Surface charge is another crucial factor influencing cellular uptake, being more efficient the higher the positive surface charge and the larger the surface-to-volume ratio of the NPs. Hence, hydrophilic NPs primarily rely on endocytosis, whereas hydrophobic NPs may associate with and penetrate the cellular membrane. Furthermore, the formation of a protein corona, resulting from the adsorption of proteins onto NP surfaces in biological fluids, significantly influences cellular interactions and is highly dependent on NP surface properties. The protein corona composition plays a vital role in modulating the NP recognition by cells, thereby impacting their uptake and subsequent intracellular fate, such as NP clearance by macrophages [12,24].

Our study showed that following dietary exposure to 1.5 mg $TiO_2$ NPs /Kg fish for 15 and 30 days, low levels of titanium were detected in the liver. Differences in the amount of titanium found in the liver of turbots exposed to both $TiO_2$ NPs might be related to the cellular uptake rate for each tested NP. $TiO_2$ NPs are naturally hydrophilic due to their negative net surface charge [134], and their further functionalization with citrate coating enhances this property [34]. Furthermore, the charge density of NPs influences their entry into cells which is negatively correlated with membrane penetration and positively correlated with membrane disruption [12]. In this context, 5 nm $TiO_2$ NPs can be more prone to accumulate in the liver as their hydrodynamic size, hydrophobicity, and high charge density favour endocytosis mechanisms. Yet, high concentrations of small $TiO_2$ NPs can form aggregates, leading to their clearance by the immune system. Moreover, the formation and composition of the protein corona depend on the shape, size, surface area, and surface charge of NPs [36,104]. Hence, phagocytosis and protein corona probably contribute to the differential fate of 5 nm and 25 nm $TiO_2$ NPs, explaining the higher hepatic uptake and subsequent detection of titanium associated with 25 nm $TiO_2$ NPs.

Renal excretion was suggested as the preferred mechanism in freshwater fish when administered through intravenous injection [117]. However, the route of exposure plays a crucial role in the accumulation and excretion of nanomaterials [43]. Previous studies indicated hepatic excretion of $TiO_2$ NPs into the bile [56] and detected high levels of titanium in faeces [10,127], proposing the excretion of accumulated $TiO_2$ NPs through this route as a plausible mechanism in fish. Moreover,

analyses of liver and kidney proteomes suggested that the kidney is less affected by the intake of $TiO_2$ NPs than the liver in turbot [10]. Here, the substantial amounts of titanium found in the excrements of turbot exposed to different-sized $TiO_2$ NPs provide evidence supporting faecal excretion as a prominent route for eliminating these NPs.

### 4.2. Hepatic lipid droplets

As in mammals, the liver is responsible for basic metabolic functions in fish, such as nutrient processing and storage, and xenobiotic detoxification processes [145]. Lipid droplets (LDs) are dynamic organelles built up of neutral lipids, mainly triacylglycerol and sterol esters, making them available for energy production during starvation, phospholipid synthesis, and protect organisms from lipotoxicity and oxidative stress [102]. The increase of LDs in controls during the experiments is related to the elevated membrane demands as fish grow and, therefore, the need for phospholipid synthesis [102]. However, hepatocytes of turbots exposed to 25 nm $TiO_2$ NPs had fewer and smaller LDs with time, suggesting an increment in lipid catabolism [44]. In contrast, the larger LDs detected in response to 5 nm $TiO_2$ NPs point to the emergence of steatosis, hepatocyte size increase and inflammation [48]. The different gene expression patterns verified in the distinct experiments (described below) may be linked to the changes observed in the cellular LD content.

### 4.3. Oxidative stress, inflammation, and immunity

Oxidative stress and inflammatory responses to NP exposure have been discussed often in the literature (revised in [61,84]). It has been suggested that $TiO_2$ NPs enter the cells and enhance the generation of ROS, affecting the oxidative stress response mediated by NRF2 and the NFκB1 signalling pathway and damaging DNA, proteins, lipids, and carbohydrates [83].

NRF2 is a transcription factor that regulates redox homeostasis inducing the expression of detoxification enzymes and endogenous antioxidants to prevent genome instability caused by oxidative stressors [28]. Although not statistically significant, our findings suggest a possible trend towards a decrease in the expression of *nrf2* in the liver of turbots exposed to small $TiO_2$ NPs. This decrease can lead to DNA damage, ultimately to apoptosis, as previously reported in Nrf2 knockout mice [121]. Compared to smaller NPs, exposure to citrate-coated 25 nm $TiO_2$ NPs resulted in a slight increase in *nrf2* expression levels, indicating that turbots were able to trigger an antioxidant response under these conditions. A previous study reported no significant changes in the expression of *nrf2* in the rainbow trout liver cell line RTL-W1 exposed for 24 h up to 100 μg/mL of 25 nm $TiO_2$ NPs stabilized with bovine serum albumin (BSA), having highlighted a protective effect of BSA against the production of ROS [78]. Conversely, the exposure of Nile tilapia (*Oreochromis niloticus*) to 10 mg/L of 25 nm $TiO_2$ NPs for 14 days has significantly decreased the NRF2 protein content in the liver, as well as the activity of antioxidant enzymes [137]. These studies provide evidence of the importance of the NP protein corona influencing physicochemical properties (size, shape, and hydrophobicity), internalization and *in vivo* fate (stability, targeting capacity, pharmacokinetics, and toxicity) of NPs [146]. The opposite responses to the $TiO_2$ NPs tested here confirm that NPs with the same coating may interact with distinct biomolecules and possibly vary in the protein corona composition and consequently exhibit different mechanisms of uptake, reactive oxygen species production, and cellular toxicity [52].

The NFκB signalling pathway is crucial for survival and is activated by ROS, ultraviolet radiations, cytokines [interleukine-1 (IL-1) and tumour necrosis factor α (TNF-α)], and microbial components. NFκB is a family of inducible transcription factors, composed of NFκB1, NFκB2, RelA, RelB and c-Rel, which mediate immune and inflammatory responses and are also involved in cell proliferation, differentiation, development, and apoptosis [101]. After its activation, NFκB1 translocates to the nucleus and induces the expression of proinflammatory genes, such as cytokines (TNF-α, IL-1, IL-6, IL-12), and cyclooxygenase-2 [82]. Previous studies have reported the activation of this pathway as a response to $TiO_2$ NPs exposure in mice [125,37,50], rats [94], as well as *in vitro* exposures in several cell lines [100,107,114,88]. In this study, the *nfκb1* expression levels significantly increased in the liver of turbots exposed to the larger $TiO_2$ NPs, consistent with previous statements suggesting that the inflammatory response is NP size-dependent [103].

Kim et al., [75] suggested that the toxicity mechanisms of citrate-coated $TiO_2$ NPs in zebrafish embryos depend more on the surface area or particle number than the overall amount of $TiO_2$ in suspension. The amounts of citrate used in our study to stabilize these NPs differed (higher in 5 nm $TiO_2$ NPs than in 25 nm $TiO_2$ NPs), which may have influenced the inflammatory response of turbots. In macrophage mitochondria, citrate can be converted into itaconate by the aconitate decarboxylase 1 (IRG1), where it inhibits succinate dehydrogenase (SDH), reducing ROS production (Fig. 4) [92]. In the cytosol, itaconate promotes the accumulation of NRF2, resulting in the transcription of antioxidant genes and the inhibition of IL-1β cytokine production (Fig. 4) [92,106]. On the other hand, itaconate inhibits IκBζ, a member of the inhibitor of NFκB (IκB) family which associates with NFκB1 homodimers in the *IL-6* gene promotor, having in turn a pleiotropic effect on the expression of NFκB target genes (Fig. 4) [70]. Overall, we raise the hypothesis that 5 nm $TiO_2$ NPs may induce the production of itaconate in the liver as a response to increased citrate ions input, prompting the NRF2 protein accumulation in cells without the need to increase *nrf2* expression. The accumulated NRF2 will trigger the expression of antioxidant genes, resulting in ROS neutralization, IL-1β reduction and consequently, a decrease of *nfκb1* expression. In contrast, 25 nm $TiO_2$ NPs will contribute to mitochondrial ROS production, increasing the amounts of NFκB1's stimuli and, therefore, the need to increase the expression of this gene.

### 4.4. Endocrine system and hormone signalling pathways

The endocrine system is responsible for the secretion and diffusion of chemical messengers over large distances and essential to physiological and biological functions [40]. Nuclear receptors (NRs) are the major components of this system, acting as receptors for chemical messengers with endogenous or exogenous sources [23,47]. In this study, we have investigated whether exposure to NPs promotes different NRs expression patterns. The different sizes of $TiO_2$ NPs induced different expression patterns of genes related to lipid metabolism, resulting in LD abundance variability despite the lack of significant changes in the expression of selected NRs under the test conditions.

The glucocorticoid receptor (GR) participates in glucose homeostasis and immune response regulation, modulating the expression of thousands of genes [128]. Interestingly, GRs have been described to interact with NFκB proteins, binding to the NFκB complex in the nucleus, inhibiting its transcriptional activity and promoting the translocation of the NFκB complex back to the cytosol, or increasing the binding affinity of IκB to NFκB complex in the cytosol, [17]. However, GR activity can be regulated by multiple mechanisms, resulting in the activation or repression of gene transcription and non-genomic effects, exercising mutually antagonistic or synergetic effects depending on the combination of stimuli [17,26]. Fish have two GR receptors, which GR1 responds to higher cortisol levels and has its expression, apart from *il-1β* and *tnf-α* genes, increased in specific sea bream tissues under stress conditions [133]. Our results did not show a significant alteration in *gr1* expression. Nevertheless, the more pronounced increase of *gr1* expression beyond the itaconate production hypothesis (Fig. 4) may explain the slight decrease of *nfκb1* expression after exposure to the smaller $TiO_2$ NPs. This finding is further supported by the lower level of *gr1* expression and the significantly higher level of *nfκb1* expression after exposure to the larger $TiO_2$ NPs.

The thyroid hormone receptors (THRs) are modulated upon binding to thyroid hormones (TH), regulating biological processes such as development, differentiation, and metabolism. In fish, THRs have been implicated in eggs development before hatching, metamorphosis during the larvae-to-juvenile transition, and organ differentiation during the

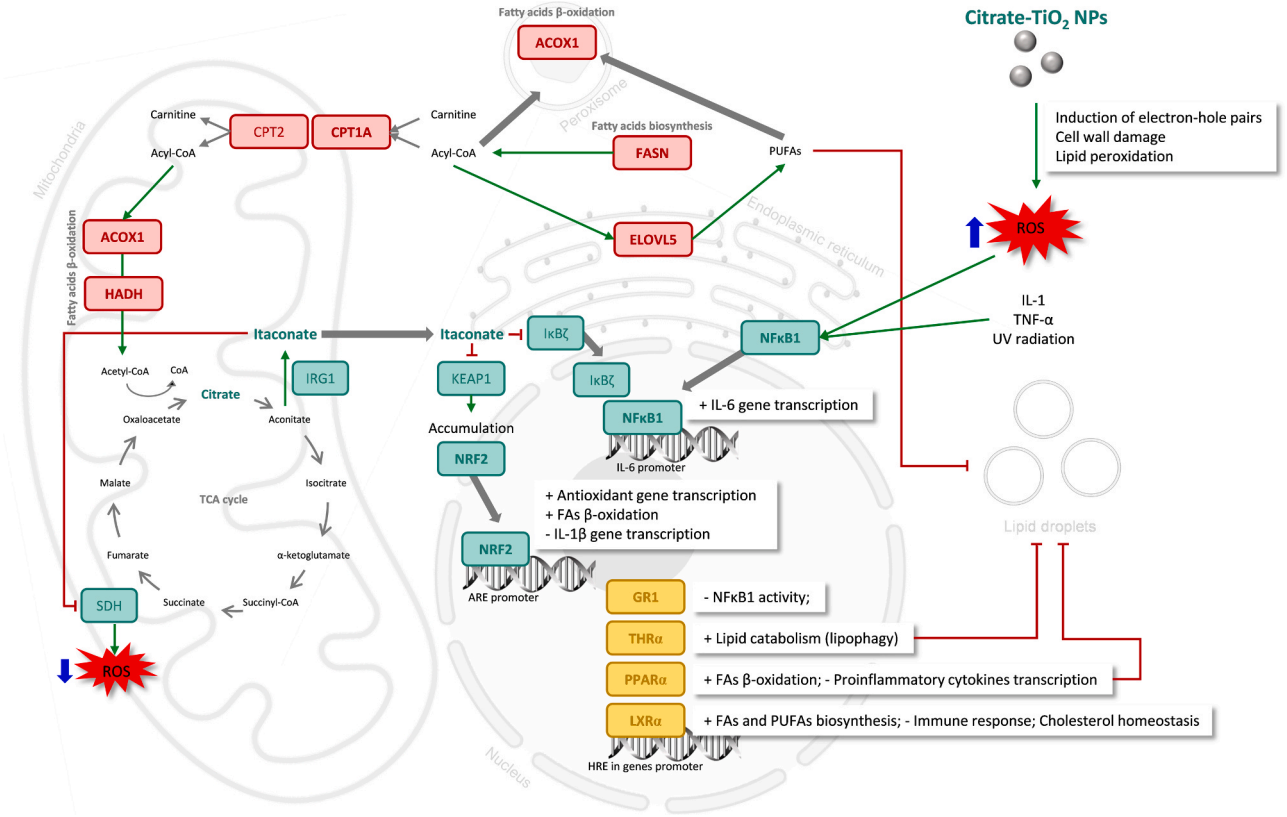


**Fig. 4.** Crosstalk among lipid metabolism, inflammatory and oxidative stress responses, and endocrine signalling pathways. Citrate-coated $TiO_2$ NPs enter the cells and induce electron-hore pairs, cell membrane damage, and lipid peroxidation, producing Reactive Oxygen Species (ROS). ROS activate the Nuclear Factor Kappa B Subunit 1 (NFκB1) which translocates to the nucleus to promote the expression of proinflammatory genes. The input of citrate ions leads to itaconate generation, inhibiting the succinate dehydrogenase (SDH) enzyme and the consequent decrease in mitochondrial ROS production. In the cytosol, itaconate interacts with the Kelch-like ECH-associated protein 1 (KEAP1), resulting in nuclear factor erythroid 2–related factor 2 (NRF2) accumulation and with the inhibitor of nuclear factor kappa B zeta (IκBζ), inhibiting it. The accumulation of NRF2 promotes the transcription of antioxidant genes, fatty acids (FAs) β-oxidation-related genes and represses the interleukin-1 beta (IL-1β) gene transcription. The inhibition of IκBζ and IL-1β gene transcription leads to the inactivation of the NFκB signalling pathway. The endocrine signalling pathways are mediated by nuclear receptors (NRs). Sensing the lipid content and its levels in cells and other small lipophilic signalling molecules, NRs (GR1, THRα, PPARα, LXRα) regulate the expression of genes related to FAs metabolism, cholesterol homeostasis, and the inflammatory and immune systems. The synthesis of FAs by FA synthase (FASN) and polyunsaturated FAs (PUFAs) by fatty acid desaturases (FADS1, FADS2), fatty acid elongases (ELOVL2, ELOVL5) promote the FAs β-oxidation and the consequent lipid droplet (LD) depletion. Green arrows indicate activation or induction; red dashes indicate inhibition; thick grey arrows indicate translocation; up and down blue arrows indicate increase and decrease, respectively.

juvenile-to-adult transition [9,110]. A previous study from our laboratory found that the amount of SERPINA7 (thyroxine and 3,5,3'-triiodothyronine blood carrier) is higher in turbots exposed to 25 nm $TiO_2$ NPs for 14 days [10], which may explain the increase of *thrαb* expression reported here to respond to THs circulating in the blood. In the liver, THs induce lipophagy releasing fatty acids for mitochondrial lipid oxidation [30]. We have observed a decrease in LDs after 30 days of exposure to 25 nm $TiO_2$ NPs that can be a consequence of lipophagy induced by THR activation on the day14 (Fig. 4), which is corroborated by the decrease in *thrαb* expression and the increase in the number and size of LDs after exposure to 5 nm $TiO_2$ NPs.

The peroxisome proliferator-activated receptors (PPARs) are crucial for energy metabolism and immunity and are modulated by lipid derivates [132]. In vertebrates, including fish, three paralogs are described as having different functions, including activation of mitochondrial and peroxisomal fatty acids β-oxidation (PPARα), glucose and fatty acids metabolism (PPARβ/δ), adipocyte differentiation energy storage (PPARγ), and inhibition of inflammatory mediators [105,126]. The expression of *pparαb* in the liver tended to increase over time in the presence of 5 nm $TiO_2$ NPs, which we suggest activates the β-oxidation of fatty acids in mitochondria to overcome the observed accumulation of lipids in LDs and protect against steatosis [126] (Fig. 4).

The liver X receptor (LXR) is a pivotal player in cholesterol homeostasis, in *de novo* fatty acid and polyunsaturated fatty acids (PUFAs) biosynthesis, and in the immune response [20,140]. The increase of PUFAs inhibits the NFκB activity, and their incorporation in phospholipids decreases membrane saturation, reducing the endoplasmic reticulum stress caused by fatty acid synthesis, [20,140]. The expression of *lxrα* tended to increase with long-term exposure to the smaller $TiO_2$ NPs, which can induce fatty acids biosynthesis and block the immune response by the increasing PUFAs. On the other hand, $TiO_2$ NPs are described to cause membrane damage due to ROS production and cholesterol is known to provide a stabilising effect [87]. In this context, boosting demand for LXRα may be necessary to regulate cholesterol homeostasis under 5 nm $TiO_2$ NPs exposure. Such hypotheses remain unclear, and there is a paucity in the literature on the role of LXRα under $TiO_2$ NP stress, unveiling the need for future research.

### 4.5. Fatty acids metabolism

Lipids, particularly fatty acids, are a crucial source of energy for the growth and health of flatfish [85]. The *de novo* biosynthesis of fatty acids in cytosol involves the rate-limiting enzyme fatty acid synthase (FASN) that produces long-chain fatty acids from acetyl-CoA and the synthesis of PUFAs in the endoplasmic reticulum that requires fatty acid desaturases (FADS1, FADS2), fatty acid elongases (ELOVL2, ELOVL5) and ultimately, peroxisomal β-oxidation [69]. In our study, the expression of

*fasn* and *elovl5* genes was not significantly affected by $TiO_2$ NPs exposure. Nevertheless, the expression of *elovl5* tended to decrease in turbots exposed to 5 nm $TiO_2$ NPs, which could lead to the alteration of the lipid content and the accumulation of LDs [67,74,95] (Fig. 4).

The catabolism of fatty acids takes place in both mitochondria (short-, medium-, and long-chain fatty acids) and peroxisome (very-long-chain fatty acids) [35]. Carnitine palmitoyl transferases (CPT1 and CPT2) are responsible for the transport of long-chain fatty acids (acyl-CoA) into the mitochondria. Acyl-coenzyme A oxidase 1 (ACOX1; peroxisomal and mitochondrial isoforms are encoded by the same gene), the first limiting-rate enzyme of this pathway, and hydroxyacyl-Coenzyme A dehydrogenase (HADH), the enzyme responsible for the oxidation of fatty acids, are then required to undergo the process of fatty acids β-oxidation [129,139] (Fig. 4). Additionally, citrate intake was reported to inhibit CPT1 [144], which is in line with our observations when turbots were exposed to higher amounts of citrate ions (5 nm $TiO_2$ NPs). After long-term exposure to these NPs, PPARαb mediated significant upregulation of *cpt1a* to defeat LD accumulation [129]. When exposed to 25 nm $TiO_2$ NPs, lipophagy was activated initially by THRα [115], resulting in a significant increase in *cpt1a* expression. Since the LD content was reduced over time, *cpt1a* expression returned to normal. The slightly high expression of *acox1* observed in the presence of $TiO_2$ NPs was expected since fatty acids β-oxidation was activated. Our results do not allow us to distinguish whether these increments affect mitochondria or peroxisome activity. We then propose that in the presence of 25 nm $TiO_2$ NPs, the changes in *acox1* expression levels primarily affect the mitochondrial isoform rather than the peroxisomal isoform, promoting lipophagy and mitochondrial fatty acid β-oxidation, ultimately leading to LDs depletion [58].

## 5. Conclusion

In summary, we presented additional evidence of lipid metabolism impairment in the liver of juvenile turbot *Scophthalmus maximus* caused by exposure to citrate-coated $TiO_2$ NPs. The ingestion of the examined NPs had a specific impact on the hepatic LD content and gene expression patterns related to lipid catabolism. While smaller NPs contributed to the accumulation of LDs in hepatocytes and subsequent steatosis, larger NPs led to the depletion of LDs in hepatocytes by lipophagy and fatty acids β-oxidation activation with a consequent increase in oxidative stress and immune responses. Our findings brought to discussion the role of the citrate coating as the mediator of such effects, highlighting the need to extend the knowledge about the risks associated with exposure to NPs with different physicochemical properties in aquatic organisms. Further studies are needed to validate these hypotheses and understand whether either different available citrate levels or corona protein composition contribute to these findings.

### *Environmental Implications*

A comprehensive examination reveals increasing amounts of titanium dioxide nanoparticles ($TiO_2$ NPs) in the environment. $TiO_2$ NPs can cause oxidative stress, histopathological alterations, immune system disturbance, and other harmful effects. We employed molecular and histological methods to understand how different sizes of $TiO_2$ NPs affect the liver of turbots over time via feeding exposure to disclose the impact of NPs in aquatic environments. Our results suggested that the severity of lipid metabolism impairment, evidenced by changes in hepatic lipid droplet size and number and altered expression of related genes, can be influenced by the citrate used as a coating agent.

### *CRediT authorship contribution statement*

**Elza Fonseca:** Methodology, Investigation, Formal analysis, Writing – original draft, Writing – review & editing. **María Vázquez:** Conceptualization, Methodology, Investigation, Formal analysis, Writing – original draft. **Laura Rodriguez-Lorenzo:** Investigation, Formal analysis, Writing – original draft, Writing – review & editing. **Natalia Mallo:** Investigation, Formal analysis, Writing – review & editing. **Ivone Pinheiro:** Investigation, Formal analysis, Writing – review & editing. **Maria Lígia Sousa:** Investigation, Writing – original draft, Writing – review & editing. **Santiago Cabaleiro:** Conceptualization, Methodology, Supervision, Writing – review & editing, Funding acquisition. **Monica Quarato:** Investigation, Formal analysis, Writing – review & editing. **Miguel Spuch-Calvar:** Investigation, Formal analysis, Writing – review & editing. **Miguel A. Correa-Duarte:** Investigation, Formal analysis, Writing – review & editing, Funding acquisition. **Juan Jose Lopez Mayan**: Methodology, Investigation, Formal analysis, Writing – review & editing. **Mick Mackey**: Conceptualization, Methodology, Writing – review & editing. **Antonio Moreda**: Conceptualization, Methodology, Formal analysis, Writing – review & editing. **Vítor Vasconcelos:** Writing – review & editing, Supervision, Funding acquisition. **Begoña Espiña:** Conceptualization, Methodology, Writing – review & editing, Supervision, Project administration, Funding acquisition. **Alexandre Campos:** Conceptualization, Methodology, Writing – review & editing, Supervision, Funding acquisition. **Mário Jorge Araújo:** Conceptualization, Methodology, Investigation, Formal analysis, Writing – original draft, Writing – review & editing, Supervision.

## Declaration of Competing Interest

The authors declare that they have no known competing financial interests or personal relationships that could have appeared to influence the work reported in this paper.

## Data Availability

Data will be made available on request.

## Acknowledgements

This work was supported by the European Regional Development Fund (ERDF) through Interreg Atlantic Area Program, project NANOCULTURE (EAPA 590/2018), and the Portuguese Foundation for the Science and Technology (FCT) (UIDB/04423/2020, UIDP/04423/2020). L.R.-L. acknowledges work contract funded by FCT (2020.04021.CEECIND). A.C. acknowledges the work contract funded by FCT (CEECIND/03767/2018). M.A.C.-D. acknowledges financial support from the Spanish Ministerio de Economía y Competitividad (PID2020-113704RB-I00), Xunta de Galicia/FEDER (IN607A 2018/5 and Centro Singular de Investigación de Galicia Acc. 2019-2022, ED431G 2019-06). We thank the Nanophotonics & Bioimaging and AEMIS facilities and staff at INL, and the Centre for Scientific and Technological Support to Research (CACTI) at the University of Vigo for their contribution.

## Appendix A. Supporting information

Supplementary data associated with this article can be found in the online version at doi:10.1016/j.jhazmat.2023.131915.

## References

[1] Ahmad, N., Fariza, M., Azman, T., Khairul, A.M., Zafirah, M.I.A., Nurliyana, M.A., 2021. Fabrication and characterization of p-Cu2O on n-TiO2 layer by electrodeposition method for heterojunction solar cells development. J Hum Earth Future 2 (4), 334–344. https://doi.org/10.28991/HEF-2021-02-04-02.

[2] Ahmad, N.S., Abdullah, N., Yasin, F.M., 2020. Toxicity assessment of reduced graphene oxide and titanium dioxide nanomaterials on gram-positive and gram-negative bacteria under normal laboratory lighting condition. Toxicol Rep 7, 693–699. https://doi.org/10.1016/j.toxrep.2020.04.015.

[3] Akhavan, O., Ghaderi, E., 2009. Photocatalytic reduction of graphene oxide nanosheets on TiO 2 thin film for photoinactivation of bacteria in solar light irradiation. J Phys Chem C 113 (47), 20214–20220. https://doi.org/10.1021/jp906325q.

[4] Akhavan, O., Ghaderi, E., 2010. Toxicity of graphene and graphene oxide nanowalls against bacteria. ACS Nano 4 (10), 5731–5736. https://doi.org/10.1021/nn101390x.

[5] Akhavan, O., Ghaderi, E., 2013. Flash photo stimulation of human neural stem cells on graphene/TiO2 heterojunction for differentiation into neurons. Nanoscale 5 (21), 10316. https://doi.org/10.1039/c3nr02161k.

[6] Allegri, M., Bianchi, M.G., Chiu, M., Varet, J., Costa, A.L., Ortelli, S., et al., 2016. Shape-related toxicity of titanium dioxide nanofibres. PLoS One 11 (3), e0151365. https://doi.org/10.1371/journal.pone.0151365.

[7] Amde, M., Liu, J., Tan, Z.-Q., Bekana, D., 2017. Transformation and bioavailability of metal oxide nanoparticles in aquatic and terrestrial environments. A review. Environ Pollut 230, 250–267. https://doi.org/10.1016/j.envpol.2017.06.064.

[8] ANSES. (2019). *Avis de l'Agence nationale de sécurité sanitaire de l'alimentation, de l'environnement et du travail relatif au risques liés à la ingestion de l'additif alimentaire E171 . Saisine n° 2019-SA-0036.* ⟨https://www.anses.fr/fr/system/files/ERCA2019SA0036.pdf⟩.

[9] Araújo, M.J., Quintaneiro, C., Rocha, R.J.M., Pousão-Ferreira, P., Candeias-Mendes, A., Soares, A.M.V.M., et al., 2022. Single and combined effects of ultraviolet radiation and triclosan during the metamorphosis of Solea senegalensis. Chemosphere 307, 135583. https://doi.org/10.1016/j.chemosphere.2022.135583.

[10] Araújo, M.J., Sousa, M.L., Fonseca, E., Felpeto, A.B., Martins, J.C., Vázquez, M., et al., 2022. Proteomics reveals multiple effects of titanium dioxide and silver nanoparticles in the metabolism of turbot, Scophthalmus maximus. Chemosphere 308, 136110. https://doi.org/10.1016/j.chemosphere.2022.136110.

[11] Auclair, J., Turcotte, P., Gagnon, C., Peyrot, C., Wilkinson, K.J., Gagné, F., 2019. The influence of surface coatings on the toxicity of silver nanoparticle in rainbow trout. Comp Biochem Physiol Part C: Toxicol Pharmacol 226, 108623. https://doi.org/10.1016/j.cbpc.2019.108623.

[12] Azhdarzadeh, M., Saei, A.A., Sharifi, S., Hajipour, M.J., Alkilany, A.M., Sharifzadeh, M., et al., 2015. Nanotoxicology: advances and pitfalls in research methodology. Nanomedicine 10 (18), 2931–2952. https://doi.org/10.2217/nnm.15.130.

[13] Azimzada, A., Jreije, I., Hadioui, M., Shaw, P., Farner, J.M., Wilkinson, K.J., 2021. Quantification and characterization of Ti-, Ce-, and Ag-nanoparticles in global surface waters and precipitation. Environ Sci Technol 55 (14), 9836–9844. https://doi.org/10.1021/acs.est.1c00488.

[14] Balzar, D., 1993. X-ray diffraction line broadening: modeling and applications to high-Tc superconductors. J Res Natl Inst Stand Technol 98 (3), 321. https://doi.org/10.6028/jres.098.026.

[15] Baranowska-Wójcik, E., Szwajgier, D., Oleszczuk, P., Winiarska-Mieczan, A., 2020. Effects of titanium dioxide nanoparticles exposure on human health—a review. Biol Trace Elem Res 193 (1), 118–129. https://doi.org/10.1007/s12011-019-01706-6.

[16] Behzadi, S., Serpooshan, V., Tao, W., Hamaly, M.A., Alkawareek, M.Y., Dreaden, E.C., et al., 2017. Cellular uptake of nanoparticles: journey inside the cell. Chem Soc Rev 46 (14), 4218–4244. https://doi.org/10.1039/C6CS00636A.

[17] Bekhbat, M., Rowson, S.A., Neigh, G.N., 2017. Checks and balances: the glucocorticoid receptor and NFκB in good times and bad. Front Neuroendocrinol 46, 15–31. https://doi.org/10.1016/j.yfrne.2017.05.001.

[18] Belekbir, S., El Azzouzi, M., El Hamidi, A., Rodríguez-Lorenzo, L., Santaballa, J. A., Canle, M., 2020. Improved photocatalyzed degradation of phenol, as a model pollutant, over metal-impregnated nanosized TiO2. Nanomaterials 10 (5), 996. https://doi.org/10.3390/nano10050996.

[19] Benson, D.A., Cavanaugh, M., Clark, K., Karsch-Mizrachi, I., Lipman, D.J., Ostell, J., et al., 2012. GenBank. Nucleic Acids Res 41 (D1), D36–D42. https://doi.org/10.1093/nar/gks1195.

[20] Bilotta, M.T., Petillo, S., Santoni, A., Cippitelli, M., 2020. Liver X receptors: regulators of cholesterol metabolism, inflammation, autoimmunity, and cancer. Front Immunol *11*. https://doi.org/10.3389/fimmu.2020.584303.

[21] Bischoff, N.S., de Kok, T.M., Sijm, D.T.H.M., van Breda, S.G., Briedé, J.J., Castenmiller, J.J.M., et al., 2020. Possible adverse effects of food additive E171 (Titanium Dioxide) related to particle specific human toxicity, including the immune system. Int J Mol Sci 22 (1), 207. https://doi.org/10.3390/ijms22010207.

[22] Blanca, M., Alarcón, R., Arnau, J., Bono, R., Bendayan, R., 2017. Non-normal data: Is ANOVA still a valid option? Psicothema 29 (4), 552–557. https://doi.org/10.7334/psicothema2016.383.

[23] Bookout, A., Jeong, Y., Downes, M., Yu, R., Evans, R., Mangelsdorf, D., 2006. Anatomical profiling of nuclear receptor expression reveals a hierarchical transcriptional network. Cell 126 (4), 789–799. https://doi.org/10.1016/j.cell.2006.06.049.

[24] Borgognoni, C.F., Mormann, M., Qu, Y., Schäfer, M., Langer, K., Öztürk, C., et al., 2015. Reaction of human macrophages on protein corona covered TiO2 nanoparticles. Nanomed: Nanotechnol, Biol Med 11 (2), 275–282. https://doi.org/10.1016/j.nano.2014.10.001.

[25] Cao, X., Han, Y., Gu, M., Du, H., Song, M., Zhu, X., et al., 2020. Foodborne titanium dioxide nanoparticles induce stronger adverse effects in obese mice than non-obese mice: gut microbiota dysbiosis, colonic inflammation, and proteome alterations. Small 16 (36), 2001858. https://doi.org/10.1002/smll.202001858.

[26] Caratti, G., Matthews, L., Poolman, T., Kershaw, S., Baxter, M., Ray, D., 2015. Glucocorticoid receptor function in health and disease. Clin Endocrinol 83 (4), 441–448. https://doi.org/10.1111/cen.12728.

[27] Carmo, T.L.L., Siqueira, P.R., Azevedo, V.C., Tavares, D., Pesenti, E.C., Cestari, M. M., et al., 2019. Overview of the toxic effects of titanium dioxide nanoparticles in blood, liver, muscles, and brain of a Neotropical detritivorous fish. Environ Toxicol 34 (4), 457–468. https://doi.org/10.1002/tox.22699.

[28] Chen, C.-H., 2020. Nrf2-ARE pathway: defense against oxidative stress. Xenobiotic Metabolic Enzymes: Bioactivation and Antioxidant Defense. Springer International Publishing, pp. 145–154. https://doi.org/10.1007/978-3-030-41679-9_13.

[29] Chen, Y., Wang, Z., Xu, M., Wang, X., Liu, R., Liu, Q., et al., 2014. Nanosilver incurs an adaptive shunt of energy metabolism mode to glycolysis in tumor and nontumor cells. ACS Nano 8 (6), 5813–5825. https://doi.org/10.1021/nn500719m.

[30] Chi, H.-C., Tsai, C.-Y., Tsai, M.-M., Yeh, C.-T., Lin, K.-H., 2019. Molecular functions and clinical impact of thyroid hormone-triggered autophagy in liver-related diseases. J Biomed Sci 26 (1), 24. https://doi.org/10.1186/s12929-019-0517-x.

[31] Choi, H.C., Jung, Y.M., Kim, S.Bin, 2005. Size effects in the Raman spectra of TiO2 nanoparticles. Vib Spectrosc 37 (1), 33–38. https://doi.org/10.1016/j.vibspec.2004.05.006.

[32] Chow, J.C.L., 2021. Synthesis and applications of functionalized nanoparticles in biomedicine and radiotherapy. Additive Manufacturing with Functionalized Nanomaterials. Elsevier, pp. 193–218. https://doi.org/10.1016/B978-0-12-823152-4.00001-6.

[33] Chu, Z., Zhang, S., Zhang, B., Zhang, C., Fang, C.-Y., Rehor, I., et al., 2014. Unambiguous observation of shape effects on cellular fate of nanoparticles. Sci Rep 4 (1), 4495. https://doi.org/10.1038/srep04495.

[34] Connolly, M., Hernández-Moreno, D., Conde, E., Garnica, A., Navas, J.M., Torrent, F., et al., 2022. Influence of citrate and PEG coatings on the bioaccumulation of TiO2 and CeO2 nanoparticles following dietary exposure in rainbow trout. Environ Sci Eur 34 (1), 1. https://doi.org/10.1186/s12302-021-00581-0.

[35] Console, L., Scalise, M., Giangregorio, N., Tonazzi, A., Barile, M., Indiveri, C., 2020. The link between the mitochondrial fatty acid oxidation derangement and kidney injury. Front Physiol *11*. https://doi.org/10.3389/fphys.2020.00794.

[36] Corbo, C., Molinaro, R., Parodi, A., Toledano Furman, N.E., Salvatore, F., Tasciotti, E., 2016. The impact of nanoparticle protein corona on cytotoxicity, immunotoxicity and target drug delivery. Nanomedicine 11 (1), 81–100. https://doi.org/10.2217/nnm.15.188.

[37] Cui, Y., Liu, H., Zhou, M., Duan, Y., Li, N., Gong, X., et al., 2011. Signaling pathway of inflammatory responses in the mouse liver caused by TiO2 nanoparticles. J Biomed Mater Res Part A 96A (1), 221–229. https://doi.org/10.1002/jbm.a.32976.

[38] Cunha, I., Galante-Oliveira, S., Rocha, E., Planas, M., Urbatzka, R., Castro, L.F.C., 2013. Dynamics of PPARs, fatty acid metabolism genes and lipid classes in eggs and early larvae of a teleost. Comp Biochem Physiol Part B: Biochem Mol Biol 164 (4), 247–258. https://doi.org/10.1016/j.cbpb.2013.01.003.

[39] Dhupal, M., Oh, J.-M., Tripathy, D.R., Kim, S.-K., Koh, S.B., Park, K.-S., 2018. Immunotoxicity of titanium dioxide nanoparticles via simultaneous induction of apoptosis and multiple toll-like receptors signaling through ROS-dependent SAPK/JNK and p38 MAPK activation. Int J Nanomed Volume 13, 6735–6750. https://doi.org/10.2147/IJN.S176087.

[40] Diamanti-Kandarakis, E., Bourguignon, J.P., Giudice, L.C., Hauser, R., Prins, G.S., Soto, A.M., et al., 2009. Endocrine-disrupting chemicals: an endocrine society scientific statement. *Endocr Rev* Vol. 30 (4). https://doi.org/10.1210/er.2009-0002.

[41] Diniz, M.S., de Matos, A.P.A., Lourenço, J., Castro, L., Peres, I., Mendonça, E., et al., 2013. Liver alterations in two freshwater fish species (*Carassius auratus* and *Danio rerio*) following exposure to different TiO $_2$ nanoparticle concentrations. Microsc Microanal 19 (5), 1131–1140. https://doi.org/10.1017/S1431927613013238.

[42] Dorier, M., Tisseyre, C., Dussert, F., Béal, D., Arnal, M.-E., Douki, T., et al., 2019. Toxicological impact of acute exposure to E171 food additive and TiO2 nanoparticles on a co-culture of Caco-2 and HT29-MTX intestinal cells. Mutat Res/Genet Toxicol Environ Mutagen 845, 402980. https://doi.org/10.1016/j.mrgentox.2018.11.004.

[43] Dube, E., Okuthe, G.E., 2023. Engineered nanoparticles in aquatic systems: toxicity and mechanism of toxicity in fish. Emerg Contam 9 (2), 100212. https://doi.org/10.1016/j.emcon.2023.100212.

[44] Ducharme, N.A., Bickel, P.E., 2008. Minireview: lipid droplets in lipogenesis and lipolysis. Endocrinology 149 (3), 942–949. https://doi.org/10.1210/en.2007-1713.

[45] EFSA, Younes, M., Aquilina, G., Castle, L., Engel, K., Fowler, P., et al., 2021. Safety assessment of titanium dioxide (E171) as a food additive. EFSA J 19 (5). https://doi.org/10.2903/j.efsa.2021.6585.

[46] Fatima, S., Ali, K., Ahmed, B., Al Kheraif, A.A., Syed, A., Elgorban, A.M., et al., 2021. Titanium dioxide nanoparticles induce inhibitory effects against planktonic cells and biofilms of human oral cavity isolates of rothia mucilaginosa, georgenia sp. and staphylococcus saprophyticus. Pharmaceutics 13 (10), 1564. https://doi.org/10.3390/pharmaceutics13101564.

[47] Fonseca, E., Machado, A.M., Vilas-Arrondo, N., Gomes-Dos-Santos, A., Veríssimo, A., Esteves, P., et al., 2020. Cartilaginous fishes offer unique insights into the evolution of the nuclear receptor gene repertoire in gnathostomes. Gen Comp Endocrinol 295, 113527. https://doi.org/10.1016/j.ygcen.2020.113527.

[48] Gluchowski, N.L., Becuwe, M., Walther, T.C., Farese, R.V., 2017. Lipid droplets and liver disease: from basic biology to clinical implications. Nat Rev Gastroenterol Hepatol 14 (6), 343–355. https://doi.org/10.1038/nrgastro.2017.32.

[49] Gondikas, A.P., Kammer, F., von der, Reed, R.B., Wagner, S., Ranville, J.F., Hofmann, T., 2014. Release of TiO2 nanoparticles from sunscreens into surface waters: a one-year survey at the old danube recreational lake. Environ Sci Technol 48 (10), 5415–5422. https://doi.org/10.1021/es405596y.
[50] Gui, S., Zhang, Z., Zheng, L., Cui, Y., Liu, X., Li, N., et al., 2011. Molecular mechanism of kidney injury of mice caused by exposure to titanium dioxide nanoparticles. J Hazard Mater 195, 365–370. https://doi.org/10.1016/j.jhazmat.2011.08.055.
[51] Hajareh Haghighi, F., Mercurio, M., Cerra, S., Salamone, T.A., Bianymotlagh, R., Palocci, C., et al., 2023. Surface modification of TiO $_2$ nanoparticles with organic molecules and their biological applications. J Mater Chem B 11 (11), 2334–2366. https://doi.org/10.1039/D2TB02576K.
[52] Hajipour, M.J., Raheb, J., Akhavan, O., Arjmand, S., Mashinchian, O., Rahman, M., et al., 2015. Personalized disease-specific protein corona influences the therapeutic impact of graphene oxide. Nanoscale 7 (19), 8978–8994. https://doi.org/10.1039/C5NR00520E.
[53] Hall, S., Bradley, T., Moore, J.T., Kuykindall, T., Minella, L., 2009. Acute and chronic toxicity of nano-scale TiO $_2$ particles to freshwater fish, cladocerans, and green algae, and effects of organic and inorganic substrate on TiO $_2$ toxicity. Nanotoxicology 3 (2), 91–97. https://doi.org/10.1080/17435390902788078.
[54] Hamilton, R.F., Wu, N., Porter, D., Buford, M., Wolfarth, M., Holian, A., 2009. Particle length-dependent titanium dioxide nanomaterials toxicity and bioactivity. Part Fibre Toxicol 6 (1), 35. https://doi.org/10.1186/1743-8977-6-35.
[55] Hammond, S.A., Carew, A.C., Helbing, C.C., 2013. Evaluation of the effects of titanium dioxide nanoparticles on cultured Rana catesbeiana tailfin tissue. Front Genet *4*. https://doi.org/10.3389/fgene.2013.00251.
[56] Handy, R.D., Henry, T.B., Scown, T.M., Johnston, B.D., Tyler, C.R., 2008. Manufactured nanoparticles: their uptake and effects on fish—a mechanistic analysis. Ecotoxicology 17 (5), 396–409. https://doi.org/10.1007/s10646-008-0205-1.
[57] Hashemi, E., Akhavan, O., Shamsara, M., Rahighi, R., Esfandiar, A., Tayefeh, A. R., 2014. Cyto and genotoxicities of graphene oxide and reduced graphene oxide sheets on spermatozoa. RSC Adv 4 (52), 27213. https://doi.org/10.1039/c4ra01047g.
[58] He, A., Dean, J.M., Lu, D., Chen, Y., Lodhi, I.J., 2020. Hepatic peroxisomal β-oxidation suppresses lipophagy via RPTOR acetylation and MTOR activation. Autophagy 16 (9), 1727–1728. https://doi.org/10.1080/15548627.2020.1797288.
[59] Helmlinger, J., Sengstock, C., Groß-Heitfeld, C., Mayer, C., Schildhauer, T.A., Köller, M., et al., 2016. Silver nanoparticles with different size and shape: equal cytotoxicity, but different antibacterial effects. RSC Adv 6 (22), 18490–18501. https://doi.org/10.1039/C5RA27836H.
[60] Holzwarth, U., Gibson, N., 2011. The Scherrer equation versus the 'Debye-Scherrer equation', 534–534 Nat Nanotechnol 6 (9). https://doi.org/10.1038/nnano.2011.145.
[61] Hou, J., Wang, L., Wang, C., Zhang, S., Liu, H., Li, S., et al., 2019. Toxicity and mechanisms of action of titanium dioxide nanoparticles in living organisms. J Environ Sci 75, 40–53. https://doi.org/10.1016/j.jes.2018.06.010.
[62] IARC Working Group, 2010. Carbon black, titanium dioxide, and talc. IARC Monogr Eval Carcinog. Risks Hum. 93, 1–413.
[63] Jaiswal, S., Manhas, A., Pandey, A.K., Priya, S., Sharma, S.K., 2022. Engineered nanoparticle-protein interactions influence protein structural integrity and biological significance. Nanomaterials 12 (7), 1214. https://doi.org/10.3390/nano12071214.
[64] Jannesari, M., Akhavan, O., Madaah Hosseini, H.R., Bakhshi, B., 2020. Graphene/CuO $_2$ nanoshuttles with controllable release of oxygen nanobubbles promoting interruption of bacterial respiration. ACS Appl Mater Interfaces 12 (32), 35813–35825. https://doi.org/10.1021/acsami.0c05732.
[65] Jannesari, M., Akhavan, O., Madaah Hosseini, H.R., Bakhshi, B., 2023. Oxygen-rich graphene/ZnO2-Ag nanoframeworks with pH-switchable catalase/peroxidase activity as O2 nanobubble-self generator for bacterial inactivation. J Colloid Interface Sci 637, 237–250. https://doi.org/10.1016/j.jcis.2023.01.079.
[66] Jiang, X., Manawan, M., Feng, T., Qian, R., Zhao, T., Zhou, G., et al., 2018. Anatase and rutile in evonik aeroxide P25: Heterojunctioned or individual nanoparticles? Catal Today 300, 12–17. https://doi.org/10.1016/j.cattod.2017.06.010.
[67] Jonas, W., Schwerbel, K., Zellner, L., Jähnert, M., Gottmann, P., Schürmann, A., 2022. Alterations of lipid profile in livers with impaired lipophagy. Int J Mol Sci 23 (19), 11863. https://doi.org/10.3390/ijms231911863.
[68] Jovanović, B., Ji, T., Palić, D., 2011. Gene expression of zebrafish embryos exposed to titanium dioxide nanoparticles and hydroxylated fullerenes. Ecotoxicol Environ Saf 74 (6), 1518–1525. https://doi.org/10.1016/j.ecoenv.2011.04.012.
[69] Jump, D.B., 2011. Fatty acid regulation of hepatic lipid metabolism. Curr Opin Clin Nutr Metab Care 14 (2), 115–120. https://doi.org/10.1097/MCO.0b013e328342991c.
[70] Kamata, H., Tsuchiya, Y., Asano, T., 2010. IκBβ is a positive and negative regulator of NF-κB activity during inflammation. Cell Res 20 (11), 1178–1180. https://doi.org/10.1038/cr.2010.147.
[71] Kędziora, A., Speruda, M., Krzyżewska, E., Rybka, J., Łukowiak, A., Bugla-Płoskońska, G., 2018. Similarities and differences between silver ions and silver in nanoforms as antibacterial agents. Int J Mol Sci 19 (2), 444. https://doi.org/10.3390/ijms19020444.
[72] Khan, I., Saeed, K., Khan, I., 2019. Nanoparticles: properties, applications and toxicities. Arab J Chem 12 (7), 908–931. https://doi.org/10.1016/j.arabjc.2017.05.011.
[73] Khosravi-Katuli, K., Prato, E., Lofrano, G., Guida, M., Vale, G., Libralato, G., 2017. Effects of nanoparticles in species of aquaculture interest. Environ Sci Pollut Res 24 (21), 17326–17346. https://doi.org/10.1007/s11356-017-9360-3.
[74] Kieu, T.-L.-V., Pierre, L., Derangère, V., Perrey, S., Truntzer, C., Jalil, A., et al., 2022. Downregulation of Elovl5 promotes breast cancer metastasis through a lipid-droplet accumulation-mediated induction of TGF-β receptors. Cell Death Dis 13 (9), 758. https://doi.org/10.1038/s41419-022-05209-6.
[75] Kim, M.-S., Louis, K.M., Pedersen, J.A., Hamers, R.J., Peterson, R.E., Heideman, W., 2014. Using citrate-functionalized TiO2 nanoparticles to study the effect of particle size on zebrafish embryo toxicity. Analyst 139 (5), 964. https://doi.org/10.1039/c3an01966g.
[76] Kumar, A., Pandey, A.K., Singh, S.S., Shanker, R., Dhawan, A., 2011. Engineered ZnO and TiO2 nanoparticles induce oxidative stress and DNA damage leading to reduced viability of Escherichia coli. Free Radic Biol Med 51 (10), 1872–1881. https://doi.org/10.1016/j.freeradbiomed.2011.08.025.
[77] Lakshmanan, V., Roy, R., Halim, M., 2015. Innovative process for the production of titanium dioxide. In: Lakshmanan, V.I., Roy, R., Ramachandran, V. (Eds.), Innovative Process Development in Metallurgical Industry: Concept to Commission. Springer. https://doi.org/10.1007/978-3-319-21599-0.
[78] Lammel, T., Mackevica, A., Johansson, B.R., Sturve, J., 2019. Endocytosis, intracellular fate, accumulation, and agglomeration of titanium dioxide (TiO2) nanoparticles in the rainbow trout liver cell line RTL-W1. Environ Sci Pollut Res 26 (15), 15354–15372. https://doi.org/10.1007/s11356-019-04856-1.
[79] Lei, L., Qiao, K., Guo, Y., Han, J., Zhou, B., 2020. Titanium dioxide nanoparticles enhanced thyroid endocrine disruption of pentachlorophenol rather than neurobehavioral defects in zebrafish larvae. Chemosphere 249, 126536. https://doi.org/10.1016/j.chemosphere.2020.126536.
[80] Lentzen, M., Jahnen, B., Jia, C.L., Thust, A., Tillmann, K., Urban, K., 2002. High-resolution imaging with an aberration-corrected transmission electron microscope. Ultramicroscopy 92 (3–4), 233–242. https://doi.org/10.1016/S0304-3991(02)00139-0.
[81] Liao, F., Chen, L., Liu, Y., Zhao, D., Peng, W., Wang, W., et al., 2019. The size-dependent genotoxic potentials of titanium dioxide nanoparticles to endothelial cells. Environ Toxicol 34 (11), 1199–1207. https://doi.org/10.1002/tox.22821.
[82] Liu, T., Zhang, L., Joo, D., Sun, S.-C., 2017. NF-κB signaling in inflammation. Signal Transduct Target Ther 2 (1), 17023. https://doi.org/10.1038/sigtrans.2017.23.
[83] Long, T.C., Tajuba, J., Sama, P., Saleh, N., Swartz, C., Parker, J., et al., 2007. Nanosize titanium dioxide stimulates reactive oxygen species in brain microglia and damages neurons in vitro. Environ Health Perspect 115 (11), 1631–1637. https://doi.org/10.1289/ehp.10216.
[84] Luo, Z., Li, Z., Xie, Z., Sokolova, I.M., Song, L., Peijnenburg, W.J.G.M., et al., 2020. Rethinking nano-TiO2 safety: overview of toxic effects in humans and aquatic animals. Small 16 (36), 2002019. https://doi.org/10.1002/smll.202002019.
[85] Ma, X., Bi, Q., Kong, Y., Xu, H., Liang, M., Mai, K., et al., 2022. Dietary lipid levels affected antioxidative status, inflammation response, apoptosis and microbial community in the intestine of juvenile turbot (Scophthalmus maximus L.). Comp Biochem Physiol Part A: Mol Integr Physiol 264, 111118. https://doi.org/10.1016/j.cbpa.2021.111118.
[86] Ma, Y., Zhang, J., Yu, N., Shi, J., Zhang, Y., Chen, Z., et al., 2023. Effect of nanomaterials on gut microbiota. Toxics 11 (4), 384. https://doi.org/10.3390/toxics11040384.
[87] Malekkhaiat Häffner, S., Parra-Ortiz, E., Skoda, M.W.A., Saerbeck, T., Browning, K.L., Malmsten, M., 2021. Composition effects on photooxidative membrane destabilization by TiO2 nanoparticles. J Colloid Interface Sci 584, 19–33. https://doi.org/10.1016/j.jcis.2020.09.046.
[88] Mancuso, F., Arato, I., Di Michele, A., Antognelli, C., Angelini, L., Bellucci, C., et al., 2022. Effects of titanium dioxide nanoparticles on porcine prepubertal sertoli cells: an "in vitro" study. Front Endocrinol *12*. https://doi.org/10.3389/fendo.2021.751915.
[89] Markowska-Szczupak, A., Endo-Kimura, M., Paszkiewicz, O., Kowalska, E., 2020. Are titania photocatalysts and titanium implants safe? Review on the toxicity of titanium compounds. Nanomaterials 10 (10), 2065. https://doi.org/10.3390/nano10102065.
[90] Mbanga, O., Cukrowska, E., Gulumian, M., 2022. Dissolution of titanium dioxide nanoparticles in synthetic biological and environmental media to predict their biodurability and persistence. Toxicol Vitr 84, 105457. https://doi.org/10.1016/j.tiv.2022.105457.
[91] Meena, R., Paulraj, R., 2012. Oxidative stress mediated cytotoxicity of TiO2 nano anatase in liver and kidney of Wistar rat. Toxicol Environ Chem 94 (1), 146–163. https://doi.org/10.1080/02772248.2011.638441.
[92] Mills, E.L., Ryan, D.G., Prag, H.A., Dikovskaya, D., Menon, D., Zaslona, Z., et al., 2018. Itaconate is an anti-inflammatory metabolite that activates Nrf2 via alkylation of KEAP1. Nature 556 (7699), 113–117. https://doi.org/10.1038/nature25986.
[93] Miranda, R.R., Damaso da Silveira, A.L.R., de Jesus, I.P., Grötzner, S.R., Voigt, C. L., Campos, S.X., et al., 2016. Effects of realistic concentrations of TiO2 and ZnO nanoparticles in Prochilodus lineatus juvenile fish. Environ Sci Pollut Res 23 (6), 5179–5188. https://doi.org/10.1007/s11356-015-5732-8.
[94] Mohammed, E.T., Safwat, G.M., 2020. Grape seed proanthocyanidin extract mitigates titanium dioxide nanoparticle (TiO2-NPs)–induced hepatotoxicity

through TLR-4/NF-κB signaling pathway. Biol Trace Elem Res 196 (2), 579–589. https://doi.org/10.1007/s12011-019-01955-5.
[95] Moon, Y.-A., Hammer, R.E., Horton, J.D., 2009. Deletion of ELOVL5 leads to fatty liver through activation of SREBP-1c in mice. J Lipid Res 50 (3), 412–423. https://doi.org/10.1194/jlr.M800383-JLR200.
[96] Moore, T.L., Rodriguez-Lorenzo, L., Hirsch, V., Balog, S., Urban, D., Jud, C., et al., 2015. Nanoparticle colloidal stability in cell culture media and impact on cellular interactions. Chem Soc Rev 44 (17), 6287–6305. https://doi.org/10.1039/C4CS00487F.
[97] Morais, S., 2017. The physiology of taste in fish: potential implications for feeding stimulation and gut chemical sensing. Rev Fish Sci Aquac 25 (2), 133–149. https://doi.org/10.1080/23308249.2016.1249279.
[98] Musial, J., Krakowiak, R., Mlynarczyk, D.T., Goslinski, T., Stanisz, B.J., 2020. Titanium dioxide nanoparticles in food and personal care products—what do we know about their safety? Nanomaterials 10 (6), 1110. https://doi.org/10.3390/nano10061110.
[99] Nematov, D.D., Kholmurodov, K.T., Husenzoda, M.A., Lyubchyk, A., Burhonzoda, A.S., 2022. Molecular adsorption of H2O on TiO2 and TiO2:Y surfaces. J Hum Earth Future 3 (2), 213–222. https://doi.org/10.28991/HEF-2022-03-02-07.
[100] Nica, I.C., Stan, M.S., Popescu, R.G., Nicula, N., Ducu, R., Diamandescu, L., et al., 2021. Fe-N Co-doped titanium dioxide nanoparticles induce cell death in human lung fibroblasts in a p53-independent manner. Int J Mol Sci 22 (17), 9627. https://doi.org/10.3390/ijms22179627.
[101] Oeckinghaus, A., Ghosh, S., 2009. The NF- B family of transcription factors and its regulation. a000034–a000034 Cold Spring Harb Perspect Biol 1 (4). https://doi.org/10.1101/cshperspect.a000034.
[102] Olzmann, J.A., Carvalho, P., 2019. Dynamics and functions of lipid droplets. Nat Rev Mol Cell Biol 20 (3), 137–155. https://doi.org/10.1038/s41580-018-0085-z.
[103] Padmanabhan, J., Kyriakides, T.R., 2015. Nanomaterials, inflammation, and tissue engineering. WIREs Nanomed Nanobiotechnol 7 (3), 355–370. https://doi.org/10.1002/wnan.1320.
[104] Park, S.J., 2020. Protein–nanoparticle interaction: corona formation and conformational changes in proteins on nanoparticles. Int J Nanomed Volume 15, 5783–5802. https://doi.org/10.2147/IJN.S254808.
[105] Páscoa, I., Fonseca, E., Ferraz, R., Machado, A.M., Conrado, F., Ruivo, R., et al., 2022. The preservation of PPARγ genome duplicates in some teleost lineages: insights into lipid metabolism and xenobiotic exploitation. Genes 13 (1), 107. https://doi.org/10.3390/genes13010107.
[106] Peace, C.G., O'Neill, L.A.J., 2022. The role of itaconate in host defense and inflammation. J Clin Investig 132 (2). https://doi.org/10.1172/JCI148548.
[107] Pérez-Arizti, J.A., Ventura-Gallegos, J.L., Galván Juárez, R.E., Ramos-Godinez, M., del, P., Colín-Val, Z., et al., 2020. Titanium dioxide nanoparticles promote oxidative stress, autophagy and reduce NLRP3 in primary rat astrocytes. Chem-Biol Interact 317, 108966. https://doi.org/10.1016/j.cbi.2020.108966.
[108] Peters, R.J.B., van Bemmel, G., Herrera-Rivera, Z., Helsper, H.P.F.G., Marvin, H.J.P., Weigel, S., et al., 2014. Characterization of titanium dioxide nanoparticles in food products: analytical methods to define nanoparticles. J Agric Food Chem 62 (27), 6285–6293. https://doi.org/10.1021/jf5011885.
[109] Pfaffl, M.W., 2001. A new mathematical model for relative quantification in real-time RT-PCR. Nucleic Acids Res 29 (9), 45e–445e. https://doi.org/10.1093/nar/29.9.e45.
[110] Power, D.M., Llewellyn, L., Faustino, M., Nowell, M.A., Björnsson, B.T., Einarsdottir, I.E., et al., 2001. Thyroid hormones in growth and development of fish. Comp Biochem Physiol Part C: Toxicol Pharmacol 130 (4), 447–459. https://doi.org/10.1016/S1532-0456(01)00271-X.
[111] Powers, C.M., Slotkin, T.A., Seidler, F.J., Badireddy, A.R., Padilla, S., 2011. Silver nanoparticles alter zebrafish development and larval behavior: distinct roles for particle size, coating and composition. Neurotoxicol Teratol 33 (6), 708–714. https://doi.org/10.1016/j.ntt.2011.02.002.
[112] Prasad, R.Y., Wallace, K., Daniel, K.M., Tennant, A.H., Zucker, R.M., Strickland, J., et al., 2013. Effect of treatment media on the agglomeration of titanium dioxide nanoparticles: impact on genotoxicity, cellular interaction, and cell cycle. ACS Nano 7 (3), 1929–1942. https://doi.org/10.1021/nn302280n.
[113] Rodríguez-Ibarra, C., Medina-Reyes, E.I., Déciga-Alcaraz, A., Delgado-Buenrostro, N.L., Quezada-Maldonado, E.M., Ispanixtlahuatl-Meráz, O., et al., 2022. Food grade titanium dioxide accumulation leads to cellular alterations in colon cells after removal of a 24-hour exposure. Toxicology 478, 153280. https://doi.org/10.1016/j.tox.2022.153280.
[114] Sarikhani, M., Vaghefi Moghaddam, S., Firouzamandi, M., Hejazy, M., Rahimi, B., Moeini, H., et al., 2022. Harnessing rat derived model cells to assess the toxicity of TiO2 nanoparticles. J Mater Sci: Mater Med 33 (5), 41. https://doi.org/10.1007/s10856-022-06662-7.
[115] Sayre, N.L., Lechleiter, J.D., 2012. Fatty acid metabolism and thyroid hormones. Curr Trends Endocrinol *6*.
[116] Schmider, E., Ziegler, M., Danay, E., Beyer, L., Bühner, M., 2010. Is it really robust? Methodology 6 (4), 147–151. https://doi.org/10.1027/1614-2241/a000016.
[117] Scown, T.M., van Aerle, R., Johnston, B.D., Cumberland, S., Lead, J.R., Owen, R., et al., 2009. High doses of intravenously administered titanium dioxide nanoparticles accumulate in the kidneys of rainbow trout but with no observable impairment of renal function. Toxicol Sci 109 (2), 372–380. https://doi.org/10.1093/toxsci/kfp064.
[118] Shabbir, S., Kulyar, M.F.-A., Bhutta, Z.A., Boruah, P., Asif, M., 2021. Toxicological consequences of titanium dioxide nanoparticles (TiO2NPs) and their jeopardy to human population. BioNanoScience 11 (2), 621–632. https://doi.org/10.1007/s12668-021-00836-3.
[119] Shakeel, M., Jabeen, F., Qureshi, N.A., Fakhr-e-Alam, M., 2016. Toxic effects of titanium dioxide nanoparticles and titanium dioxide bulk salt in the liver and blood of male sprague-dawley rats assessed by different assays. Biol Trace Elem Res 173 (2), 405–426. https://doi.org/10.1007/s12011-016-0677-4.
[120] Shi, H., Magaye, R., Castranova, V., Zhao, J., 2013. Titanium dioxide nanoparticles: a review of current toxicological data. Part Fibre Toxicol 10 (1), 15. https://doi.org/10.1186/1743-8977-10-15.
[121] Shi, Z., Niu, Y., Wang, Q., Shi, L., Guo, H., Liu, Y., et al., 2015. Reduction of DNA damage induced by titanium dioxide nanoparticles through Nrf2 in vitro and in vivo. J Hazard Mater 298, 310–319. https://doi.org/10.1016/j.jhazmat.2015.05.043.
[122] Silva, P.V., Pinheiro, C., Morgado, R.G., Verweij, R.A., van Gestel, C.A.M., Loureiro, S., 2022. Bioaccumulation but no biomagnification of silver sulfide nanoparticles in freshwater snails and planarians. Sci Total Environ 808, 151956. https://doi.org/10.1016/j.scitotenv.2021.151956.
[123] Simonin, M., Richaume, A., Guyonnet, J.P., Dubost, A., Martins, J.M.F., Pommier, T., 2016. Titanium dioxide nanoparticles strongly impact soil microbial function by affecting archaeal nitrifiers. Sci Rep 6 (1), 33643. https://doi.org/10.1038/srep33643.
[124] Slomberg, D.L., Auffan, M., Guéniche, N., Angeletti, B., Campos, A., Borschneck, D., et al., 2020. Anthropogenic release and distribution of titanium dioxide particles in a river downstream of a nanomaterial manufacturer industrial site. Front Environ Sci *8*. https://doi.org/10.3389/fenvs.2020.00076.
[125] Sun, Q., Tan, D., Ze, Y., Sang, X., Liu, X., Gui, S., et al., 2012. Pulmotoxicological effects caused by long-term titanium dioxide nanoparticles exposure in mice. J Hazard Mater 235–236, 47–53. https://doi.org/10.1016/j.jhazmat.2012.05.072.
[126] Takada, I., Makishima, M., 2020. Peroxisome proliferator-activated receptor agonists and antagonists: a patent review (2014-present). Expert Opin Ther Pat 30 (1), 1–13. https://doi.org/10.1080/13543776.2020.1703952.
[127] Tang, T., Zhang, Z., Zhu, X., 2019. Toxic Effects of TiO2 NPs on Zebrafish. Int J Environ Res Public Health 16 (4), 523. https://doi.org/10.3390/ijerph16040523.
[128] Timmermans, S., Souffriau, J., Libert, C., 2019. A general introduction to glucocorticoid biology. *Front Immunol* Vol. 10 (Ju;y). https://doi.org/10.3389/fimmu.2019.01545.
[129] Todisco, S., Santarsiero, A., Convertini, P., De Stefano, G., Gilio, M., Iacobazzi, V., et al., 2022. PPAR alpha as a metabolic modulator of the liver: role in the pathogenesis of nonalcoholic steatohepatitis (NASH). Biology 11 (5), 792. https://doi.org/10.3390/biology11050792.
[130] Tovar-Sánchez, A., Sánchez-Quiles, D., Basterretxea, G., Benedé, J.L., Chisvert, A., Salvador, A., et al., 2013. Sunscreen products as emerging pollutants to coastal waters. PLoS One 8 (6), e65451. https://doi.org/10.1371/journal.pone.0065451.
[131] Tucci, P., Porta, G., Agostini, M., Dinsdale, D., Iavicoli, I., Cain, K., et al., 2013. Metabolic effects of TiO2 nanoparticles, a common component of sunscreens and cosmetics, on human keratinocytes. e549–e549 Cell Death Dis 4 (3). https://doi.org/10.1038/cddis.2013.76.
[132] Tyagi, S., Sharma, S., Gupta, P., Saini, A., Kaushal, C., 2011. The peroxisome proliferator-activated receptor: a family of nuclear receptors role in various diseases. J Adv Pharm Technol Res 2 (4), 236. https://doi.org/10.4103/2231-4040.90879.
[133] Vallejos-Vidal, E., Sanz-Milián, B., Teles, M., Reyes-Cerpa, S., Mancera, J.M., Tort, L., et al., 2022. The gene expression profile of the glucocorticoid receptor 1 (gr1) but not gr2 is modulated in mucosal tissues of gilthead sea bream (Sparus aurata) exposed to acute air-exposure stress. Front Mar Sci *9*. https://doi.org/10.3389/fmars.2022.977719.
[134] Vieira, A., Rodríguez-Lorenzo, L., Leonor, I.B., Reis, R.L., Espiña, B., dos Santos, M.B., 2023. Innovative antibacterial, photocatalytic, titanium dioxide microstructured surfaces based on bacterial adhesion enhancement. ACS Appl Bio Mater 6 (2), 754–764. https://doi.org/10.1021/acsabm.2c00956.
[135] Vignardi, C.P., Hasue, F.M., Sartório, P.V., Cardoso, C.M., Machado, A.S.D., Passos, M.J.A.C.R., et al., 2015. Genotoxicity, potential cytotoxicity and cell uptake of titanium dioxide nanoparticles in the marine fish Trachinotus carolinus (Linnaeus, 1766). Aquat Toxicol 158, 218–229. https://doi.org/10.1016/j.aquatox.2014.11.008.
[136] Vineeth Kumar, C.M., Karthick, V., Kumar, V.G., Inbakandan, D., Rene, E.R., Suganya, K.S.U., et al., 2022. The impact of engineered nanomaterials on the environment: release mechanism, toxicity, transformation, and remediation. Environ Res 212, 113202. https://doi.org/10.1016/j.envres.2022.113202.
[137] Vineetha, V.P., Devika, P., Prasitha, K., Anilkumar, T.V., 2021. Tinospora cordifolia ameliorated titanium dioxide nanoparticle-induced toxicity via regulating oxidative stress-activated MAPK and NRF2/Keap1 signaling pathways in Nile tilapia (Oreochromis niloticus). Comp Biochem Physiol Part C: Toxicol Pharmacol 240, 108908. https://doi.org/10.1016/j.cbpc.2020.108908.
[138] Vishvakarma, V., Kaur, M., Nagpal, M., Arora, S., 2023. Role of nanotechnology in taste masking: recent updates. Curr Drug Res Rev 15 (1), 1–14. https://doi.org/10.2174/2589977514666220526091259.
[139] Vluggens, A., Andreoletti, P., Viswakarma, N., Jia, Y., Matsumoto, K., Kulik, W., et al., 2010. Functional significance of the two ACOX1 isoforms and their crosstalks with PPARα and RXRα. Lab Investig 90 (5), 696–708. https://doi.org/10.1038/labinvest.2010.46.
[140] Wang, B., Tontonoz, P., 2018. Liver X receptors in lipid signalling and membrane homeostasis. Nat Rev Endocrinol 14 (8), 452–463. https://doi.org/10.1038/s41574-018-0037-x.

[141] Wang, J., Ma, J., Dong, L., Hou, Y., Jia, X., Niu, X., et al., 2013. Effect of anatase TiO $_2$ nanoparticles on the growth of RSC-364 rat synovial cell. J Nanosci Nanotechnol 13 (6), 3874–3879. https://doi.org/10.1166/jnn.2013.7145.

[142] Wang, Z., Yin, L., Zhao, J., Xing, B., 2016. Trophic transfer and accumulation of TiO2 nanoparticles from clamworm (Perinereis aibuhitensis) to juvenile turbot (Scophthalmus maximus) along a marine benthic food chain. Water Res 95, 250–259. https://doi.org/10.1016/j.watres.2016.03.027.

[143] Wani, M.R., Shadab, G., 2020. Titanium dioxide nanoparticle genotoxicity: a review of recent in vivo and in vitro studies. Toxicol Ind Health 36 (7), 514–530. https://doi.org/10.1177/0748233720936835.

[144] Williams, N.C., O'Neill, L.A.J., 2018. A role for the krebs cycle intermediate citrate in metabolic reprogramming in innate immunity and inflammation. Front Immunol *9*. https://doi.org/10.3389/fimmu.2018.00141.

[145] Wolf, J.C., Wolfe, M.J., 2005. A brief overview of nonneoplastic hepatic toxicity in fish. Toxicol Pathol 33 (1), 75–85. https://doi.org/10.1080/01926230590890187.

[146] Xiao, Q., Zoulikha, M., Qiu, M., Teng, C., Lin, C., Li, X., et al., 2022. The effects of protein corona on in vivo fate of nanocarriers. Adv Drug Deliv Rev 186, 114356. https://doi.org/10.1016/j.addr.2022.114356.

[147] Yu, C., Kim, S., Jang, M., Park, C.M., Yoon, Y., 2021. Occurrence and removal of engineered nanoparticles in drinking water treatment and wastewater treatment processes: a review, 210339–0 Environ Eng Res 27 (5). https://doi.org/10.4491/eer.2021.339.

[148] Yu, Z., Li, Q., Wang, J., Yu, Y., Wang, Y., Zhou, Q., et al., 2020. Reactive oxygen species-related nanoparticle toxicity in the biomedical field. Nanoscale Res Lett 15 (1), 115. https://doi.org/10.1186/s11671-020-03344-7.